OPTIMUM DESIGN OF COMPOSITE HYDROGEN PRESSURE VESSELS BY STOCHASTIC SEARCH METHODS

A Thesis Submitted to
the Graduate School of Engineering and Sciences of
İzmir Institute of Technology
in Partial Fulfillment of the Requirements for the Degree of

MASTER OF SCIENCE

in Mechanical Engineering

by
Abdülmecit Harun Sayı

July 2018
İZMİR

We approve the thesis of **Abdülmecit Harun SAYI**

Examining Committee Members:

Assoc. Prof. Dr. H. Seçil ARTEM
Department of Mechanical Engineering, Izmir Institute of Technology

Prof. Dr. M. Evren TOYGAR
Department of Mechanical Engineering, Dokuz Eylül University

Assist. Prof. Dr. Sinan KANDEMİR
Department of Mechanical Engineering, Izmir Institute of Technology

9 July 2018

Assoc. Prof. Dr. H. Seçil ARTEM
Supervisor, Department of
Mechanical Engineering

Prof. Dr. Metin TANOĞLU
Head of the Department of
Mechanical Engineering

Prof. Dr. Aysun SOFUOĞLU
Dean of the Graduate School
of Engineering and Sciences

ACKNOWLEDGEMENTS

I would like to express my sincere gratitude to my supervisor Assos. Prof. Dr. H. Seçil Artem for her advises guidance, support, encouragement, and inspiration through the thesis. Her patience and kindness are greatly appreciated. I have been fortunate to have Dr. Artem as my advisor and I consider it an honor working with her.

I would like to thank also Dr. Levent Aydın for his guidance, support and encouragement, which made my dissertation a better work.

I am grateful for grant #215M182 project provided by The Scientific and Technological Research Council of Turkey (TÜBİTAK). My thesis study being a part of this project was made possible thanks to this grant.

I am also grateful to my friends Ozan Ayakdaş, Melih Savran and Dr. H. Arda Deveci for their encouragements, collaboration and contributions.

I would like to thank my family who have supported and encouraged me during my graduate studies.

Lastly, I would like to thank my hobby; cycling which always clears and opens my mind and brings me health, strength, wellbeing, encouragement, discipline and motivation.

ABSTRACT

OPTIMUM DESIGN OF COMPOSITE HYDROGEN PRESSURE VESSELS BY STOCHASTIC SEARCH METHODS

Fiber-reinforced composite materials are extensively used in many engineering applications such as aircraft wings and frames, vehicle drive shafts, sport equipment, and pressure storage vessels. One of the reasons for the extensive use of laminated composite materials is their tailorable nature, which allows them to satisfy specific design objectives in an application. As an application, hydrogen-powered fuel cell vehicles require high amount of hydrogen to increase distance range. Hence, hydrogen is pressurized at elevated rates. Since, it is hard to satisfy safety and weight regulations for high pressure gas, composite storage vessels offering high strength with low weight are preferred. Optimization techniques are applied to the design of composite pressure vessels to maximize strength with comprising weight restrictions. In the thesis, first-ply failure optimizations of stacking sequence design of cylindrical composite pressure vessels with metal liner having 700-bar working pressure and safety factor of 2.0, have been performed using stochastic search algorithms which are Differential Evolution and Nelder Mead. Three separately categorized failure theories; Tsai-Wu, Maximum Stress and Hashin-Rotem criteria have been incorporated to failure analysis of the vessel designs. In addition, the effects of volume on the stacking sequence design have been investigated. Hence, four volumetrically separated pressure vessel designs have been considered. Change in volume has been provided by inner radius. Single objective optimization has been set to minimize failure criteria index which incorporates into classical lamination theory. Fiber orientation angles and number of plies are design variables. CPU time has been calculated to compare the workloads of algorithms. In conclusion, optimized pressure vessels have provided design targets and the difference in volume has caused variable fiber angle orientations, number of plies and CPU time.

ÖZET

STOKASTİK ARAMA YÖNTEMLERİ İLE KOMPOZİT HİDROJEN BASINÇLI KAPLARIN OPTİMUM TASARIMI

Günümüzde fiber takviyeli polimerik kompozit malzemeler uzay ve uçak sanayii, savunma sanayi, spor ekipmanları ve ulaşım endüstrilerinde yaygın olarak kullanılmaktadır. Tez çalışmasının konusu filament sarım ile üretilen silindirik kompozit hidrojen depolama tanklarıdır. Hidrojen depolama tanklarının yakıt hücresi ile çalışan araçlarda olduğu gibi hareket halinde kullanılacağı uygulamalarda, özel güvenlik prosedürlerini ve ağırlık limitlerini sağlaması gerekmektedir. Bu sebeple hidrojen depolama tankları, yüksek mukavemetli ve düşük ağırlığa sahip karbon fiber takviyeli polimerik kompozit malzemelerden imal edilmektedir. Bu tezde, "Differential Evolution" ve "Nelder-Mead" stokastik optimizasyon algoritmaları kullanılarak, metal astarlı silindirik kompozit hidrojen depolama tanklarının dizayn ve optimizasyonu gerçekleştirilmiştir. Dizaynların mekanik analizi, klasik laminasyon teorisi ve ince cidarlı basınçlı kap teorisine dayanmaktadır. Çalışmanın amacı, ilk tabaka kırılmasını baz alan 700 bar çalışma basıncı ile 2.0 güvenlik faktörünü sağlayan tank dizaynları geliştirmektir. Bir diğer amaç ise hacim değişiminin fiber oryantasyon açısı ve tabaka sayısına etkisi incelenmiştir. Bu amaçla, 4 farklı hacme sahip silindirik kompozit depolama tank dizaynı optimize edilmiştir. Hacimdeki değişim iç yarıçap ile sağlanmıştır. Farklı olarak kategorize edilmiş Tsai-Wu, Maksimum Stres ve Hashin-Rotem kırılma kriterleri hasar analizi için kullanılmıştır. Optimizasyon işlemlerinde kırılma kriter indeksi minimize edilirken, fiber açı oryantasyonu ve tabaka sayısı değişken bırakılmıştır. Algoritmaların CPU yükünü tespit etmek için işlem zamanları hesaplanmıştır. Güvenlik katsayısını sağlayan basınçlı tankların optimizasyonu gerçekleştirilmiştir ve depolama hacmindeki değişimin fiber açı oryantasyonu, tabaka sayısı ve işlem zamanlarında değişime sebep olduğu görülmüştür.

TABLE OF CONTENTS

LIST OF FIGURES

Figure **Page**

LIST OF TABLES

Table **Page**

CHAPTER 1

INTRODUCTION

1.1. Literature Survey

Requirement of the clean and safe energy for residence, industry and transportations has increased since emissions formed by the usage of fossil fuels, has been verified as their harmful characteristic threating all living things and the earth. Renewable energies, therefore, have to see more implementation and usage to reach sustainable energy systems [1].

Solar, wind, geothermal, hydro and biomass energy production is in the scope of many countries in the next few years. These targets can be told as dynamic situation in Europe. According to the announcement from The European Union, by 2020, up to 40% of electricity is generated from renewable energy. One of the most developed countries in Europe; Germany aims to close all nuclear power plant by 2022 and produce around 50% of its electricity mainly from solar power plants and wind parks by 2030 and targets 80% until 2050 [2].

In next 30 years, such high contribution to electricity generation by wind and solar power plants will require large areas and storage batteries. Since, extra energy being generated must be stored for not ideal weather conditions; the complexity of electricity storage must be overcome. However, the solution strongly lies on political, economic and infrastructure developments. In order to generate energy via clean sources, fossil fuels are insufficient to give requirements, especially, one of the main targets are decarbonizing the whole energy sector. Therefore, efficient connection between energy production and renewable sources is an important necessity. As an overview on this connection, Figure 1 shows one of the technological options how it should be [2].

Among energy sources, hydrogen (H_2) is a strong candidate to replace commonly used fossil fuels since it contents the highest energy density of all common fuels by weight. However, the technology behind the production and storage of hydrogen results price increment. Today, most common method to produce hydrogen is electrolysis.

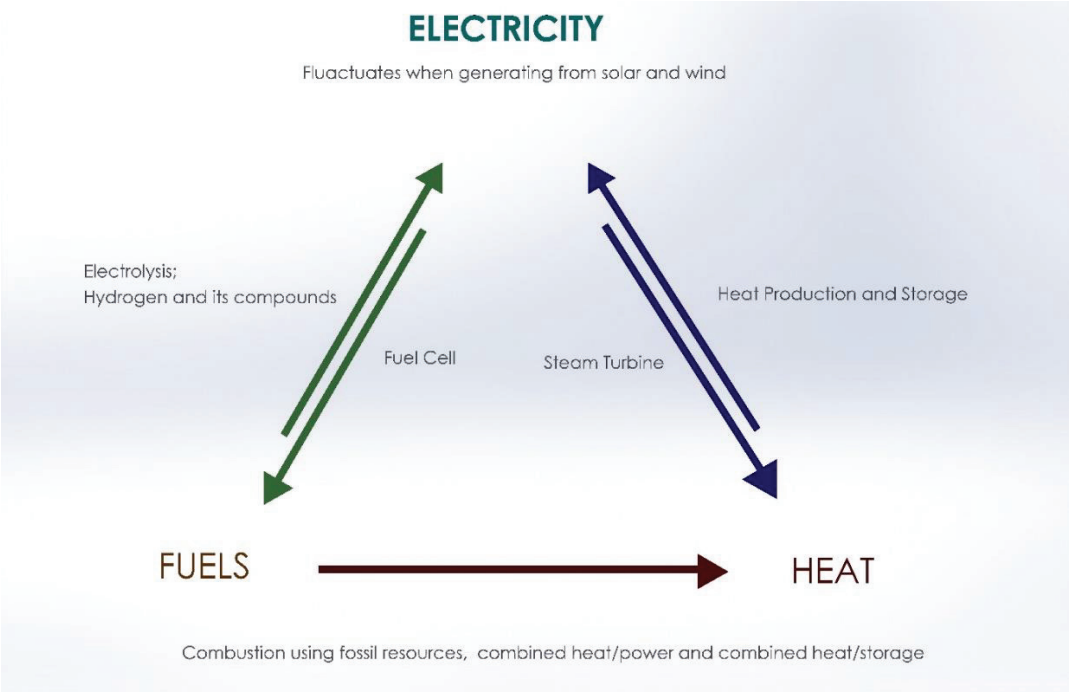

Figure 1.1 Cycle between the generation of electricity, usage of fuel and production of heat [2]

Despite recent developments in this technology [3], 1 kg of hydrogen production with electrolysis costs nearly €3 [4]. This price might decrease in time being parallel with the raising usage of hydrogen and technological developments of its production in mobile or non-mobile applications. Automobiles or in general, on-board systems being the most appealing applications of hydrogen as fuel still rely on mostly fossil fuels. If it is replaced with hydrogen, it will positively impact the usage of hydrogen and environmental targets. However, it has to be stored in a small and lightweight systems; containers or vessels due to the size and weight constraints in vehicles. In addition to its challenges, hydrogen contents lowest energy density per unit volume. Hence, there are lots of technological investments in how to store H_2 in more compact, safe, reliable, efficient and inexpensive storage options [5, 13].

Although there are certain investments on hydrogen storage, this conflict with the reality; the total global storage of hydrogen is much smaller than the total storage of natural gas. However, further integration of hydrogen storage to mobile applications presents new possibilities to ultimate safety and sustainability in future energy systems. Ideal platform to use hydrogen requires its production from renewable electricity, efficient storage and transportation and also having efficient combustion in a fuel cell or combustion chamber where the only by product is water. This closed platform is expected to form future fossil fuel free energy systems [6].

Storage of the hydrogen is one of the main subjects that engineers consider, since it is a flammable gas when it encounters with oxygen. Hence, it has to be stored in some reliable methods, before not only transportation but also storage of it in mobile applications. There are three physical hydrogen storage methods which are chemical, liquid or cryo-compressed, and compressed gas form.

In the first method, hydrogen is bonded with solids being metal hydrides which enable safe hydrogen storage at moderate pressures and temperatures. In these process, metal hydrides include metal ions which form a meshed structure where hydrogen adsorbs and being dissociated to form atomic hydrogen and it is inserted into the meshed metal structure [7, 8].

Pasini et al. [9] studied on solid state hydrogen storage, its requirements to use in vehicles and also compared them with existing metal hydride systems. According to this study, a minimum 11 wt% of storage capacity should be provided by metal hydride system in vehicle at low desorption enthalpies to reach ideal system storage density. However, currently there is no metal hydride structure which can satisfy this requirement. Today, this type of hydrogen storage system seems to have power supply to small electronics such as power banks for charging battery of electronic devices.

Liquefied hydrogen being other hydrogen storage option, has some of advantages such as more hydrogen mass in a volume and also greater energy density shown in Table 1. While excessive evaporation rate of liquid hydrogen through heat leakage from thermal insulations and connecting, parts seem to main disadvantage of this method, the real limiting factors are still the availability of the technology and cost of the liquefaction infrastructure. This phase of hydrogen can be stored with the cyro-compression technology [10]. It was first introduced by BMW in 2012[11]. It can be thought as a combination of compression and liquefaction of the hydrogen. This combination is logical method; it permits relatively high volumetric density, but it doesn’t bring solution to main problems to the system. However, if technological disadvantages are eliminated or advantages of the system are increased, it might be one of the most suitable systems to store hydrogen [12].

High pressurized hydrogen storage vessels which are the basis and focus of this study is the most common method to store hydrogen from bulk cavern storage to mobile applications such as hydrogen fuel cell vehicles. As introduced in Chapter 2, there are 4 types of hydrogen storage vessels being Type I, Type II, Type III and Type IV.

Table 1.1 Comparison of liquid and pressured hydrogen properties [10]

Property	Liquid	Gas, 300 Bar
Density	70.85 g/L	20.77 g/L
Volumetric Energy Density	2.36 kWh/L	0.69 kWh/L
Mass Energy Density	33.3 kWh/kg	33.3 kWh/kg

Since, the subject of the thesis is optimization of composite pressurized hydrogen storage vessels; the study has focused on the literature of Type III and Type IV hydrogen storage vessels.

A technical assessment of Argonne National Laboratory and Quantum Technologies supported by DOE (Department of Energy, US) have been investigated a comprehensive research and development on compressed hydrogen storage vessel systems for automotive applications. Type IV storage systems have been selected to perform mechanical and cost models. Their study enabled them to scale and design pressure vessels having varied sizes to provide 5.6 kg of usable hydrogen as oppose the typical pressure vessels having smaller storage capacity being used previously. The Benedict-Webb-Rubin Equation of state has been used to measure the amount of stored of H_2 for 5.6 kg of cyclable H_2 at 20 bar pressure. Netting analysis algorithm has been used to determine optimum dome shape with a helical winding pattern, thickness of the helical and hoop windings in the cylindrical section for certain maximum storage pressure and also length to diameter ratio. It should be noted that gravimetric and volumetric capacities of a pressure vessel define the most significant performance characteristics for any on board applications. Gravimetric capacity of H_2 storage vessel defines weight of the stored H_2 per system weight while volumetric capacity of H_2 storage vessel defines the amount of stored H_2 per liter of storage volume. Validation of the calculated carbon fiber weights and the volume of vessels of performance model have been performed using the analysis and data from Quantum Technologies. Models agreed within 1% for 350 bar vessels and within 10% for the vessel having 700 bar working pressure. The both 350 and 700 bar designs surpassed the DOE 2010 gravimetric target of 4.5 wt% while 350 bar vessels also satisfied the 2015 target of 5.5 wt%. In addition, the volumetric capacities of the models were 6% and 37% lower than the target of 28 g.H_2/L being scheduled by DOE and also, they were 34% and 56% lower than the DOE 2015 target of 40 g.H_2/L for 350 bar and 700 bar pressure vessel

models. Therefore, according to the results of this study, further assessments have been required to meet targets of DOE [14].

Manufacturing of cylindrically shaped pressure vessels, fuel tanks, pipes and rocket motor cases have been performed by the one of most popular and affordable technique called filament winding. Winding process varies in helical or hoop patterns depending on the requirement of strength, manufacturing process, fiber layout, machine accuracy and cost [15]. Dome sections of the filament wound composite pressure vessels generally require more material thickness with respect to overall, because of elevated stress concentrations in the location. The optimal dope shape has been studied in literature in any length to diameter ratio and boss opening to diameter ratios [16]. Filament winding across the dome section includes only helical windings while cylindrical region of the vessel can be filament winded by hoop and helical angled fibers.

Along with the development in manufacturing of the pressure vessels, mechanical (based on mechanics of composites such as classical lamination theory (CLT), thick or thin walled pressure vessels) and/or numerical analysis (finite element) have been performed in number of studies. In some studies, the optimal design of laminated composite pressure vessels has been obtained to minimize weight and maintenance costs. For example, Tauchert [17] obtained the optimum design of a composite cylindrical pressure vessel, Adali et al. [18] included strength constraint while optimizing of laminated composite pressure vessels. Reddy et al. [18,19] performed finite element analysis of pressure vessels to measure the linear and nonlinear first ply failure loads of laminated composite plates using certain failure theories. Chang [20] performed first ply failure of laminated composite pressure vessels which included both analytical and experimental approaches. Park et al. [21] performed the optimal stacking sequence to maximize strength of laminated composites subjected various loading and boundary conditions using Genetic Algorithm (GA). Kabir [22] performed a numerical analysis based on axis stress and reference conforming displacement formed by internal pressure in a hybrid metal composite pressure vessel having geodesic dome shape and variable thickness in order to compare with traditional solutions.

Kim et al. [23] performed an optimal design method of filament wound vessel subjected to inner pressure. Research team benefited from semi-geodesic path algorithm to determine the slippage and windability between fiber and vessel surface. Moreover,

prediction of filament wound structures was performed using finite element analysis (ABAQUS). An optimal design algorithm to use for a symmetric composite pressure vessel was suggested using GA based on semi-geodesic path algorithm and the results of finite element analysis. According to the results of algorithm, a Type III composite pressure vessel design having 100 mm inner radius and 1000 mm length, 2 helical layers, 9 hoop layers and aluminum liner with 1.9mm thickness was obtained weighing 4.44 kg as best solution of the study. Moreover, progressive failure analysis was included for the vessels based on FEA. Chapelle and Perreux [24] studied on the thermomechanical behavior of the cylindrical section of the Type III hydrogen storage vessel under static loading.

Pelletier and Vel [25] focused on maximum strength, stiffness and lightweight for cylindrical composite pressure vessels by determining stacking sequences and fiber volume fractions. Improved methodology was based on the elitist non-dominated sorting genetic algorithm (NSGA-II) [26, 27] and it was applied to obtain Pareto-optimal designs to conflict design objectives. They incorporated an automatic termination criterion in multi-objective genetic algorithm which is accepted as novel feature of this developed methodology. In their first model problem, maximization of the failure load with minimization of the weight of laminated composite structure under biaxial moment loadings is aimed. In other model problem, multi objective optimization for a graphite fiber reinforced epoxy composite section of cylindrical vessel has been performed for minimum mass and maximum hoop and axial rigidity. Optimization results of first case show that their algorithm was able to evolve efficient composite layers with a variation of the fiber volume fraction and in second problem case, it was found out that the nonlinearities in the Pareto-optimal design provided different ways to reach optimum solution. This enabled them to perform interchange their aims while choosing a specific design.

Zheng and Liu [28] studied on the elastic-plastic stress analysis and damage progress of the Type III cylindrical pressure vessel subjected to inner pressure and thermal residual stress. Elastic analysis was performed using CLT and elasto-plastic behaviors of the pressure vessel were executed by employing theories from plasticity; the Hencky Equation and the Power Hardening Theory. Further, a solution algorithm based on the last-ply failure criterion (ultimate failure theory) was performed to investigate the damage progress and the burst strength of the composite laminates of the

pressure vessel. Results of the study showed that increment in winding angle decrease the radial displacement and shear stress while increasing the radial stress. Principal stresses (axial and hoop) increase in the composite laminates but decrease in liner. Thermal effects increase the radial and principal stresses in the composite laminates while principal stresses decreased in the liner. Xu et al. [29] performed a study to determine the failure evolution and strength of the composite hydrogen storage vessels with a solution algorithm which was proposed to investigate the progressive damage and failure characteristics of composite laminates subjected to progressive inner pressure incorporating with certain failure theories. In the other study of research group of Liu [30], three Type III pressure vessels having different inner radius, thicknesses for liner and composite plies and winding angles were investigated based on continuum damage mechanics using explicit finite element method to predict the failure characteristics and burst pressures incorporating with Hashin damage initiation criterion.

Gentilleau et al. [31] used a 3D finite element model to compute stress fields for Type IV hydrogen storage vessel. Ghouaoula et al. [32] modeled a Type III hydrogen storage vessel with simulating the mechanical response of the structure to a quasi-static loading to predict damage behavior. Francescato et al. [33] established a more definitive design rule covering classical plate theory (CPT) with gradual damage and optimization and a finite element method with Reddy's progressive damage law with GA to compare optimal design methods for Type III pressure storage tanks. Kumar and Kumari [34] performed a design of the Geodesic dome of a composite pressure vessel using Geodesic Path Equation and predicted operating and failure conditions of the geodesic dome portion using CLT and finite element analysis.

Alcantar et al. [35] proposed two algorithms being GA and Simulated Annealing (SA) to optimize Type III pressure vessels having 100 mm of inner radius, 10 lt of capacity, 700 bar working pressure and a safety factor of 2.35. The main objective of the study was to minimize weight of the vessel under internal pressure where the thicknesses of the composite plies were the design variables. The results obtained from optimization were used for pressure vessel analysis by finite element. According to the results of the optimization, SA obtained minimum thickness leading less weight compared to GA. In addition, optimization with SA algorithm reduced the weight of the pressure vessel by 7.1% more than the study done using adaptive genetic algorithm previously [36]. Finite element analysis of the pressure vessel using the data obtained

by SA algorithm showed that the pressure vessel supported the working pressure while maintaining a safety factor of 2.35 which was higher value than indicated. In the other study of Alcantar and his collogues [37] performed similar study for Type IV composite pressure vessels. The optimization with GA reduced weight by 9.8% for the Type IV pressure vessel having 260 mm of inner radius while the optimization performed by SA algorithm reduced weight of 11.2% for the pressure vessel having 195 mm of inner radius compared to the solutions obtained in the study of Roh [38].

1.2. Objectives

In this study, analysis and stacking sequence optimization of fiber reinforced laminated composite layers of cylindrical composite hydrogen storage vessels incorporating with failure theories have been performed by Differential Evolution and Nelder Mead optimization algorithms. Four Type III pressure vessel designs differing in volume have been considered. The volume difference between designs has been provided by only inner radius. Therefore, the length of vessels has been selected constant for designs. Composite system of the designs has been selected as carbon fiber reinforced epoxy polymer and the liner material of the designs has been chosen as aluminum 6061-T6 from the literature. Fiber orientations of each composite layer and the number of composite layers have been taken as design variables for each design. The objectives of the thesis can be given as follows;

- Investigating optimum fiber angle orientations and number of layers for the pressure vessel having different storage volume
- Minimizing number of composite layers at burst pressure for a given laminate thickness
- Comparison of stochastic search methods, Differential Evolution (DE) and Nelder Mead (NM) in terms of optimum designs and CPU times.
- Investigating the effects of using Tsai-Wu, Hashin-Rotem and Maximum Stress theories on stacking sequence design.

It should be noted that identifying ideal failure criterion isn't easy to say for any composite structures. Because, failure theories are based on prediction analysis. Therefore, their prediction might vary according to the number of parameters such as geometry, material selection, analysis method, optimization algorithm etc. However, if

one is able to compare the outputs of failure theories with experimental data for a certain design, it would be simpler to determine ideal failure theory in the event of optimization of certain composite structure.

CHAPTER 2

COMPOSITE MATERIALS AND PRESSURIZED HYDROGEN STORAGE VESSELS

2.1. Introduction

Composites are structural materials being formed by two or more individual materials which aren't soluble in each other. Generally, the component being less than the other in blend is called reinforcement and another component is called matrix. As its name implies, matrix fills all gaps which are remained from reinforcement material. Its main objective is to transmit the loads to other material where this objective is changeable with respect to application purpose and areas, and also it protects the whole structure against deformations caused by such as abrupt temperature differences, moisture, radiation and corrosion. Reinforcement material has greater mechanical properties to accommodate mechanical, thermal or moisture related stresses from external loads acting on composite structure. Carbon fiber reinforced epoxy, fiber glass reinforced polyethylene, natural fiber reinforced polyester, steel reinforced concrete, carbon nano-tube reinforced aluminum matrix can be given as composite structure examples [39].

Composite structures have been extensively used for many centuries. For example, modern concrete being made by 75% agrega, 10% cement and 15% water has been developed by Louis Vicat in 1813 while primitive versions of it was used by Egyptians to bind mud involving chaff and stone brick to improve structural integrity of pyramids in B.C. 3000 [40]. Eskimos developed a way to use moss as a reinforcing material for their ice houses. The Katana being the most famous legendary Japanese sword, Tekkan and Hachiwari, Gunsen, Tessen and Gunbai being made by multilayered Japanese steel were used by Japanese Samurai Warriors and Ninjas for centuries [41, 42]. In 1850, construction iron was placed in cement and by this way, engineers produced a well-known composite material; iron reinforced concrete while fiber glass reinforced polymer matrix composites were firstly developed and used during World War II [43].

Laminated fiber-reinforced composite materials which form the basis of composite category in usage for composite hydrogen storage vessels, have certain characteristics; low density, high specific strength and specific modulus, that make them desirable on the applications requiring high strength, high stiffness and/or rigidities with lightweight. These features are dependent on significant parameters such as material selections, stacking sequence design, number of layers, fiber volume fraction, manufacturing method and quality etc. Highly customizable nature of composites separate them from conventional isotropic materials and make them suitable and desirable material choices for engineering applications being from aerospace, automotive and marine to sports, health and cosmetic industries. Specific strength (strength/density) and specific modulus (modulus/density) being abruptly higher for composites, reveal the main separation and put composites at another level of mechanical performance against isotropic materials as shown in Figure 2.1.

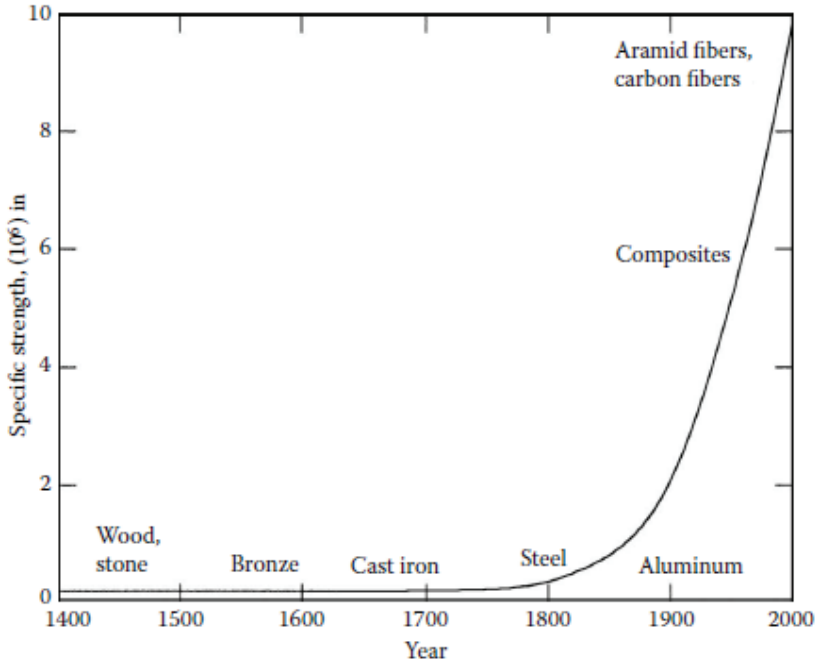

Figure 2.1 Specific strength differences between conventional and modern isotropic materials vs composites [39]

In Table 2.1, comparison of mechanical properties for fiber reinforcement materials, UD and cross-plied composites, quasi-isotropic composites and some isotropic materials has been shown [39].

Table 2.1 Density related mechanical properties comparison of several composite types, individual fibers and commonly used isotropic materials [39]

Materials	Specific Gravity	Young's Modulus (GPa)	Ultimate Strength (MPa)	Specific Modulus ($GPa.m^3/kg$)	Specific Strength ($MPa.m^3/kg$)
Graphite fiber	1.8	230	2067	0.1278	1.148
Aramid fiber	1.4	124	1379	0.08857	0.9850
Glass fiber	2.5	85	1550	0.0340	0.6200
Unidirectional graphite/epoxy	1.6	181	1500	0.1131	0.9377
Unidirectional glass/epoxy	1.8	38.60	1062	0.02144	0.5900
Cross-ply graphite/epoxy	1.6	95.98	373	0.06000	0.2331
Cross-ply glass/epoxy	1.8	23.58	88.25	0.01310	0.0490
Quasi-isotropic graphite/epoxy	1.6	69.64	276.48	0.04353	0.1728
Quasi-isotropic glass/epoxy	1.8	18.96	73.08	0.01053	0.0406
Steel	7.8	206.84	648.10	0.02652	0.08309
Aluminum	2.6	68.95	275.80	0.02652	0.1061

2.2. Classification of Composites

Composites are classified with respect to the type of matrix used such as polymer, carbon, ceramic and metal and/or the geometry of the reinforcement materials which can be particulate, flake and fibers as shown in Figure 2.2.

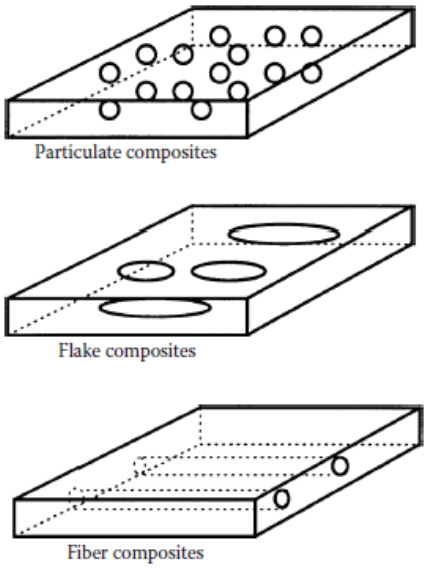

Figure 2.2 Classification of composites with respect to the geometry of its reinforcement material [39]

Composites involving particulate materials as its reinforcement material are called particulate composites. These types of materials are generally used in alloy or ceramic matrix to form composite structure. Since, random distribution of the particulate material exists, it is assumed as isotropic composites. There are certain mechanical, thermal and environmental resistance properties of these composites such as greater strength, advanced operation temperature, resistance against corrosion and moisture related deformation. Agrega and cement used to manufacture concrete, carbon nano-tube particles in epoxy composite, nano-diamond particles in aluminum matrix, aluminum particles in rubber can be given as examples [39].

Flake composites include flattened reinforcement materials compounded in matrix. Glass, mica, silver, aluminum can be used as flake type reinforcement material and the aim of type is to bring higher strength, flexural rigidity and low cost to composite structure. However, there are some disadvantages of flake composites that they cannot be easily directed and there is limited number of material which can be used as flake [39].

Being the basis composite type of this study, fiber reinforced composites are formed by fiber, matrix and the interface region. They can be named according to the fiber types which are discontinuous fiber (short type) or continuous fiber (long type). There are number of materials that can be used as fiber in composites such as glass, aramid, carbon, boron, flax, hemp etc. [39].

Polymer resins; epoxy, polyethylene, vinlyester, polyester, metals; aluminum, titanium, magnesium, ceramics; aluminum carbide, calcium-alumina silicate can be given as examples for matrix part of composites.

Laminated fiber reinforced composite materials are formed by multiple composite layers stacked together and having similar or different fiber angles to accommodate loading types of applications. By this way, properties of composite structures can be tailored according to the application areas [39]. There are also braided, knitted, non-woven, stitched and weaved continuous fiber layers being used to build laminated composite structure that have different mechanical behaviors [44].

Among all types of composites, polymer matrix composites (PMCs) are the most advanced and widely used composite types involving a polymer matrix reinforced by continuous fiber. The main reason of this preference is that PMCs provide highest strength, modulus and ease in manufacturing with lower cost. Oppositely, PMCs have

low operating temperatures, high hygrothermal expansion coefficient and low elastic properties in shear direction.

When individually examined the parts of PMCs, for example, carbon fiber mostly remains its mechanical performances at elevated temperature above 1000^{o}C, but epoxy resin begins to degrade after 200^{o}C. Hence, this causes lower mechanical performances than assumed for carbon fiber reinforced epoxy composite at elevated temperatures.

Carbon or graphite fiber and glass fiber reinforced polymer matrix composites have wide range of engineering applications. Especially in aerospace and defense industry, materials that have both high modulus and high strength with lightweight are preferred in order to produce high-end products performing better than isotropic siblings. Carbon fiber has low coefficient of thermal expansion, high fatigue strength, exceptional tensile and compression modulus and strength with certain drawbacks such as low impact resistance, low electrical insulating properties and high cost. Since the high cost restrains the usage of this material, it is also used with other cost effective fiber types such as glass or flax fiber as hybrid composite structure.

Apart from synthetic fibers, natural fibers are also preferred as reinforcing element of composites that they provide economical, technical and ecological advantages similar to synthetic fibers such as low density, high specific modulus and strength, and additionally, they are healthier, recyclable and have lower carbon emissions. Flax, jute and hemp fiber can be used as reinforcement. Comparison of different properties of carbon fiber [45, 46], glass fiber [46-11] aramid fiber [46] and natural fiber [48, 49] are indicated in Table 2.2 [45-58].

Polymer matrix divides in two categories which are thermosets; epoxies, phenolics, polyesters and polyamide and thermoplastics; polyethylene, polystyrene, PEEK (polyether–ether–ketone) and PPS (polyphenylene sulfide). Thermoset polymers include strong covalent bonds between moderate to long polymer chains resulting insoluble and infusible structure after cure, but thermoplastics have weak van der Waals bonds that permits it to be re-used. In Table 2.3, some of the different features of thermoplastics and thermosets are given [39].

Although epoxy resins are more expensive than other type of polymers, they have the most amount of usage. The advantages of epoxy matrix are high strength, low viscosity and low flow rates which bring better wetting capability to fiber without

causing misalignment during production, low evaporation during curing, low shrinkage that increase the chance to obtain lower shear stresses at interface.

Table 2.2 Comparison between various types of synthetic and natural fibers [45-58]

Properties	Carbon Fiber	Glass fiber	Aramid Fiber	Plant Fibers
Global manufacturing-Annually (metric tons)	102130	4,000,000	115,000	31,000,000
Density (g.cm^{-3})	Low (1.45)	High (~2.44-2.72)	Low (1.47)	Low (~1.35-1.55)
Tensile stiffness (GPa)	Ultra (~45-925)	Low (73)	Moderate (83-186)	Low (~30-80)
Tensile strength (GPa)	Ultra (1-7)	High (2.0-4.9)	High (3.4-4.1)	Low (~0.4-1.5)
Specific tensile stiffness (GPa/g cm^{-3})	Ultra (~137-413)	Low (27)	Moderate (~56-126)	Low (20-60)
Specific tensile strength (GPa/g cm^{-3})	Ultra (~0.7-4.8)	Moderate (~0.7-2)	High ~ (2.3-2.9)	Low (0.3-1.1)
Abrasive to machines	Yes	Yes	Yes	No
Energy consumption (MJ/kg of fibre)	High (183-450)	Moderate (30-50)	Ultra (575-1730)	Low (4-15)
Renewable source	No	No	No	Yes
Recyclable	Partly	Partly	Partly	Yes
Biodegradable	No	No	No	Yes
Toxic (upon inhalation)	Yes	Yes	Yes	No

Table 2.3 Comparison of the differences between two types of polymers [39]

Thermoplastics	Thermosets
Soften due to heat and pressure, and easy to repair	Decompose on heating
High strains to failure	Low strains to failure
Indefinite shelf life	Definite shelf life
Reprocessable	Cannot reprocessable
Not tacky and easy to handle	Tacky
Short cure cycles	Long cure cycles
Higher fabrication temperature and viscosities have made it difficult to process	Lower fabrication temperature
Fine solvent resistance	Fair solvent resistance

These features of epoxy resins allow it to be used in wide variety of engineering applications.

Carbon-carbon composites (C-C) are formed by carbon as its both reinforcement and matrix material. By this way, the exceptional mechanical properties of carbon fiber at elevated temperatures are maintained in a composite structure. However, usage of C-C composites is not common due to excessive cost, low shear strength and tendency of oxidation at elevated temperatures.

Aluminum, titanium and magnesium are common types of metals or alloys to constitute metal matrix composites (MMCs) with reinforcement materials such as carbon, boron or ceramic fibers. The aim for using metal matrix composite in an application is to bring advanced mechanical and thermal properties compared to conventional types such as higher strength, higher stiffness with lower density and lower thermal expansion coefficient.

Ceramic matrix composites (CMCs) consist of ceramic based matrices such as silicon carbide, alumina calcium, aluminum oxide, zirconia, silicon nitride with ceramic type fibers. The most important advantage of CMCs are high hardness and high service temperature. In addition, they have high strength with low density and have higher resistance against chemical based degradation. On the contrary to their hardness, their fracture toughness is much lower than conventional materials [59]. In Table 2.4, characteristics of common matrix materials are indicated and certain behaviors of the common fibers are compared in Table 2.5 [60].

Table 2.4 Characteristics of common matrix materials [60]

Property	**Metals**	**Ceramics**		**Polymers**
		Bulk	**Fibers**	
Tensile strength	+	-	++	v
Stiffness	++	v	++	-
Fracture toughness	+	-	v	+
Impact strength	+	-	v	+
Fatigue endurance	+	v	+	+
Creep	v	v	++	-
Hardness	+	+	+	-
Density	-	+	+	++
Dimensional stability	+	v	+	-
Thermal stability	v	+	++	-
Hygroscopic sensitivity	++	v	+	v
Weatherability	v	v	v	+
Erosion resistance	+	+	+	-
Corrosion Resistance	-	v	v	+
++, superior; +, good; -, poor; v, variable.				

Table 2.5 Comparison of reinforcing fibers [60]

Fiber	Advantages	Disadvantages
E-glass, S-glass	High strength Low cost	Low stiffness Short fatigue life High temperature sensitivity
Aramid (Kevlar)	High tensile strength Low density	Low compressive strength High moisture absorption
Boron	High stiffness High compressive strength	High cost
Carbon (AS4, T700, C6000)	High strength High stiffness	Moderately high cost
Graphite (GY-70, pitch)	Very high stiffness	Low strength High cost
Ceramic (silicon carbide, alumina)	High stiffness High use temperature	Low strength High cost

2.3. Application of Composite Materials

Journey of people seeking more knowledge about wide variety of things being creation of universe, space, deep oceans and also wars leads to build more advanced machines, systems and structures such as international space station, artificial satellites, space shuttles, planes, ships, submarines, tanks, armored vehicles, missiles, rockets and firearms. Technological developments in these industries positively induce the progress of other regions of human life such as more advanced buildings, bridges, sport equipment, vehicles and so on. In every development case, materials of things have always get the huge part of importance. Even though conventional materials such as steel might provide sufficient mechanical properties, they lack the properties such as low density, low thermal expansion coefficient and low corrodibility which cause, for example, the use of more powerful engine for lifting the mass and special coatings that a space shuttle requires in the event of huge thermal stresses.

NASA engineers benefit from a material system which they call it as Thermal Protection System (TPS) in their space shuttles. This system protects shuttle from heat during reenter to atmosphere and cold temperatures experienced when in space by providing a temperature range being in between -121^{o}C and 1649^{o}C. The nose cap, the nose landing gear doors and edges of the wings are made by reinforced Carbon-Carbon composite which provide the shuttle to withstand mechanical and thermal stress formed above 1260^{o}C [61].

In sport of road cycling, engineers always try to improve rigidity to weight ratio of bicycle framesets. Since, a bicycle is a human powered machine, less weight with no loss in power through frame means faster bicycles at same applied power compared to metal made examples. In order to improve structural integrity, durability and especially rigidities of bicycle frames which are usually referred to bottom bracket and head tube area, they design more robust tube geometries and use carbon fiber reinforced polymer composites. By this way, it can be possible to manufacture bike frames having more rigidity to weight ratio. It should be noted that although carbon fiber reinforced epoxy composite has greater stiffness values than aluminum alloy, it doesn't mean that individual rigidity values at certain areas will follow this. Because, the most important parameters affecting rigidity are geometry and assembly methods of each tubes of frame. Therefore, when determining the rigidity of an area, it should be looked at rigidity to weight ratio to determine rational results. The comparison of advanced road bike frames made by 6011 aluminum alloy, Toray 800 carbon fiber epoxy composite and Toray 700 carbon fiber epoxy composite can be seen in Table 2.6 accordingly weight, pedaling rigidity and steering-torsional rigidity (bike models are registered trademark of Taiwanese Giant Bicycle Company) [62]. From the table, frames made by carbon fiber reinforced composites offer more rigidity to weight ratio in average.

Table 2.6 Comparison of three similar road bikes in weights and rigidities [62]

Bike Number	**Frame Material**	**Frame Weight (g)**	**Pedaling Rigidity (N/mm)**	**Pedaling rigidity/weight ratio**	**Steering Rigidity (Nm/º)**	**Steering rigidity/ weight ratio**	**Mean of Rigidity/Weight Ratio**
1	Toray 800/Epoxy Composite	920	76.96	0.083	160.73	0.174	0.129
2	Toray 700/Epoxy Composite	968	65.91	0.068	150.8	0.156	0.112
3	6011-T6 Aluminum Alloy	1050	74.01	0.070	130.56	0.124	0.097
(It should be noted that all frame of bikes presented in table have identical geometry in medium size)							

A bicycle frameset requires high rigidity and low weight especially in the event of sprinting (quick accelerations) and climbing. According to the literature, weight

reduction is directly correlated with increment in speed while cyclist generates work against gravity too (climbing) that every 10% reduction of total system weight (bicycle, rider and luggage) requires 10% less power to maintain same speed. In a criterium race (lap based flat road race which involve lots of stop and accelerating due to sharp corners through the finish), if riders brake while cornering, the energy converts to heat. For example, a cyclist having 90 kg of mass, tries to keep the speed at 40 km/h in a typical flat course consisting of 1 km circuit, 4 corners per lap, 10km/h speed loss at each corner for 1 hour duration, will have to perform 160 accelerations after each corner. During this period, each 10% decrement in total system weight will improve power loss by 3%. Hence, the importance of material having higher strength with less weight become vital in sport of cycling in order to win a race [63].

According to the current market share, carbon fiber reinforced polymer composites (CFRP) are getting more qualified and cost effective compared to conventional materials. Since it is strongly connected with the development in materials, manufacturing and assembly technology, the cost of CFRP is reducing by these improved technologies. In Figure 2.3, cost comparison of various type of CFRP, matrix and conventional material is indicated [64].

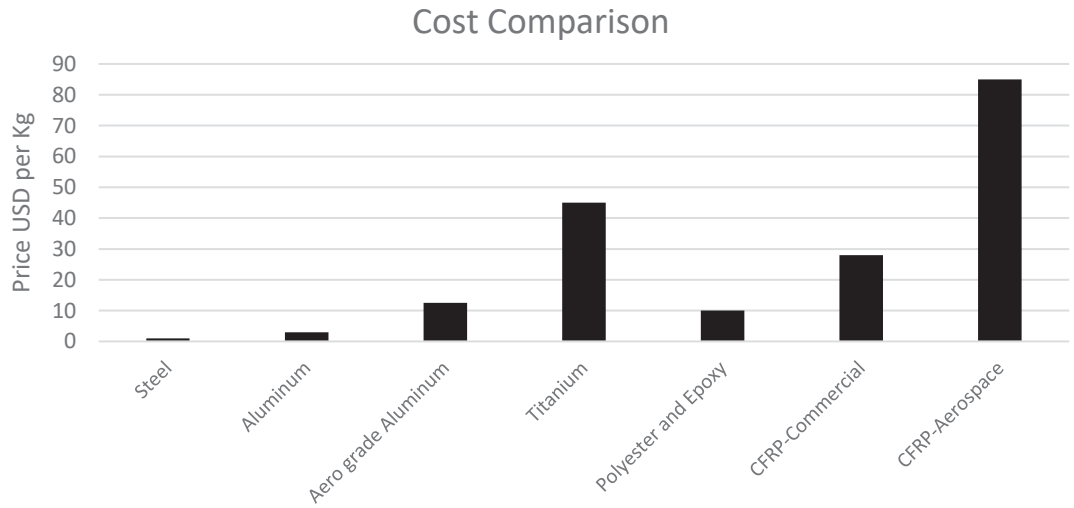

Figure 2.3 Cost comparison of CFRP, common matrices and metals [64]

According to the individual industrial demand of carbon fiber, aerospace and defense, sports, marine and transportation industries require significant portion respectively which can be seen at Figure 2.4 [64].

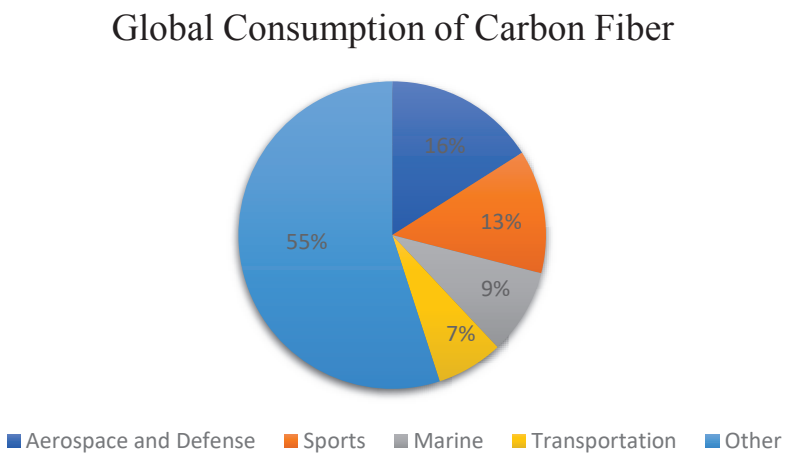

Figure 2.4 Global consumption rates of carbon fiber in certain industries [64]

However, when demand of CFRP is compared to other reinforced composite, its usage is still dramatically less than glass fiber reinforced composites seen at Figure 2.5 [65]. The main reason of this significant difference is high cost of carbon fiber that generally isolates its usage only in special applications. However, as mentioned above, due to its greater properties than glass fiber, its demand is ascending according to current rates along with the development in its production and assembly technologies which reduce the cost.

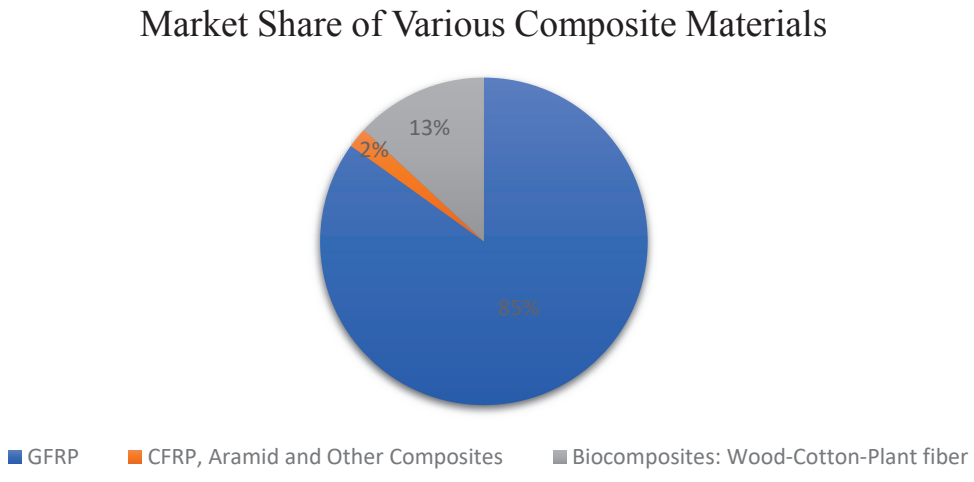

Figure 2.5 Comparison of relative market share for composites in 2010 [65]

2.3. Pressurized Hydrogen Storage Vessels

High pressurized hydrogen storage vessels which are the basis and focus of this study is one of the available method to store hydrogen from bulk cavern storage to on-board applications such as hydrogen fuel cell vehicles. Storage of hydrogen is critical issue through production, transportation and end-use application. Although hydrogen is measured to have one of the most potent fuel source, it will be vast if it isn't carried with certain safety, suitability for on-board and stationary applications. The storage of hydrogen in pressurized gaseous form is one of the most common and efficient way to carry and use this gas. To overcome the requirement of strength to accommodate high pressure, materials selected for the vessel must provide high strength and stiffness. In most applications, however, the optimization approaches are not used effectively which results excessive material usage and a rather poor assessment of the pressure vessel lifetime [66, 67].

Storage pressure of hydrogen is ranging between 200 bar and 1000 bar with respect to application area and also the type of vessel. Due to its natural properties, hydrogen gas tends to be adsorbed by surface material which causes diffusion of atomic hydrogen into material resulting loss of flexibility (embrittlement) of material. Hence, a thick/thin liner made by metal alloys (stainless steel, aluminum and rarely titanium), or polymers (HDPE: high density polyethylene), are used as inner part of composite pressure vessels [68, 69].

A pressure vessel is a system including gas container, valves to reduce excessive pressure, pipeline and sensors to adjust pressure and temperature. It has to be certificated in order to prove its usability in applications. Therefore, it undergoes certain tests and number of regulations before usage. Monitoring of pressure, temperature, tank filling level and emergency stop which are certain requirements of certain electronic safety systems are developed for especially on-board applications [70, 71].

Currently, there are four types of pressurized gas storage vessels being available to use for certain applications according to the European Integrated Hydrogen Project [73]. These types are classified as Type I, Type II, Type III and Type IV as shown in Figure 2.7.

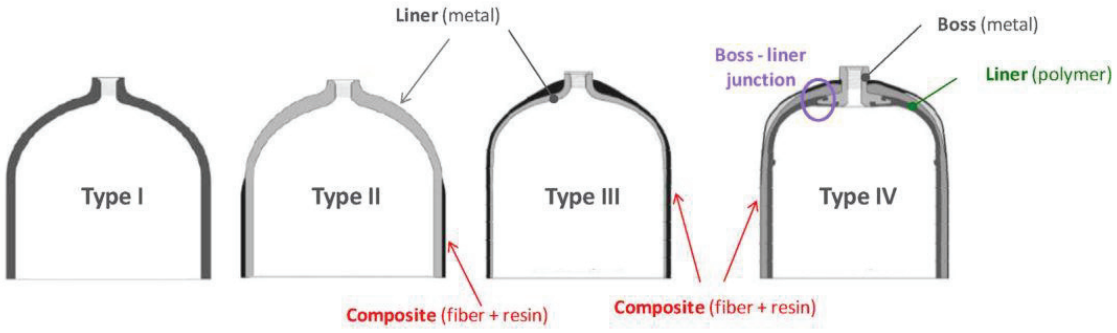

Figure 2.6 Types of pressure vessels to store hydrogen in varying working pressures [74]

Type I storage tanks are made by only thick metal alloy which is generally steel or aluminum. Being the least expensive pressurized gas storage vessel type, estimated production cost is $5 per liter of volume ranging from 2.5 to 50 lt. The pressures of Type I are between 200 and 500 bar. They are heavy and its energy density is around 0.4 kWh/kg. The requirements and labor skills to produce this type of vessel are available internationally. It is generally preferred for scuba diving, welding, fire extinguisher and ozone/oxygen rehabilitation of patients. It is not recommended to store hydrogen to use for fuel cell vehicles due to its weights being approximately 1.4 kg/L. To use pressurized hydrogen for on-board purposes, Type I storage vessels have been replaced by composite containers which provide lightweight. As mentioned above, a thin liner accompanies with composite materials to assure the gas tightness of composite pressure vessels [72].

Type II storage tanks are produced using thick metal liner; generally, steel, as its main reinforcement part and hoop wrapped composite material as its sub-reinforcement. The composite wrapped region is only cover cylindrical region of the vessel. If continuous filaments are wrapped on thin metal liner or polymer liner in both helical and hoop angles, the pressure vessels are categorized as Type III and Type IV, respectively. In these types, metal or polymer liners are not main load bearing member of the vessel. Thin liner is required to prevent hydrogen permeation and composite region ensures mechanical integrity of the vessel [73, 74]. The key characteristics of pressure vessel types are indicated in Table 2.7.

Table 2.7 The comparison of pressure vessel types with respect to technological maturity, cost and weight [75]

Category	Current Development Stage	Cost Performance	Weight Performance
Type I	P is limited to 500 bar	++	-
Type II	There is no pressure limit	+	0
Type III	Pressure is limited 450 bar – Difficult to provide standards and regulations required for 700 bar	-	+
Type IV	Pressure can be up to 1000 bar – However, the resistance of polymer liner to gas diffusion should be studied	-	++
- (under avarage), 0 (neutral), + (above average), ++ (much better than average)			

Metallic liners of Type I, Type II and Type III pressure vessel can be produced from three different methods which are by plates, billets and tubes. In first method, deep-drawing is applied to form the shape, in second method, billet is firstly heated before drawing process. For all methods, the neck of the liner is shaped by hot-spinning while the ports are processed in the excess of metal which comes from this step. Heat treatments are applied as last step to bring optimum mechanical properties to liner. Synthetic liners used in Type IV vessels are manufactured by rotomolding, blow molding or welding injection which is based on extrusion of tube shape from polymer [75].

Apart from their discrepancy in liners, other main difference between Type III and Type IV pressure vessels is load bearing capacity of liner. In Type III pressure vessels, metallic liner mechanically supports the whole structure by more than 5% while load bearing capacity of synthetic liner used in Type IV is lower than 5%. The most common metals for metallic liner are 6061-T6 or 7060 of aluminum alloys and inox or chrome molybdenum steel alloys while polyethylene or polyamide based synthetic liners are preferred for Type IV vessels. After 350 bar inner pressure, carbon fiber is

preferred to provide mechanical safety standards rather than other fiber materials being generally aramid and glass and most common matrix material are based on epoxy resins which provide good mechanical properties, compatibility with filament winding process and stability. In this case, pre-impregnated (wetting process of fiber with epoxy in resin pool before winding) fibers are preferred to reduce cost [75].

According to European Integrated Hydrogen Project, weight efficiency for on-board vehicles is set at 4.8% of hydrogen stored in a vessel. This target can only be reached by Type III and Type IV pressure vessels which achieve 700 bar or more working pressure. Typically, 6 kg of stored H_2 is necessary for a light duty vehicle which has range of 500 km. US Department of Energy (DOE) sets a target on gravimetric capacity (weight efficiency) of 5.5% and volumetric capacity of 40 g/L at operating temperature of -40 to 60^oC under delivery pressure of 12 bar. However, the volumetric capacity of most common pressure vessels is 0.089 g/L. Since 6 kg H_2 seizes a spherical volume of 5 meter in diameter, it seems impossible to produce pressure vessel for on-board applications. Currently, new generation Type III and Type IV pressure vessels provide 700 bar working pressure. However, although storage pressure increase, they need to have volume of 150 L to store 6 kg H_2. To overcome this challenge, engineers design twin or multi Type III or Type IV pressure vessels working in parallel formation. In Table 2.8, typical characteristics of Type III and Type IV pressure vessels ranging various volume and storage pressure are expressed in detail. [71, 73, 75, 76, 77].

Table 2.8 Comparison of Type III and Type IV pressure vessel characteristics

Net Volume (L)	**34**	**100**	**50**	**100**	**36**	**65**	**30**	**120**
Type	III	III	III	III	IV	IV	IV	IV
Working Pressure (bar)	350	350	700	700	350	350	700	700
Proof Test Pressure (bar)	525	525	1050	1050	525	525	1050	1050
System Weight (kg)	18	48	55	95	18	33	26	84
Volume (L)	50	150	80	150	60	100	60	200

cont. on next page

Table 2.8 **(cont.)**

H_2 Density (kg/m^3) at 25°C	23.3	23.3	39.3	39.3	23.3	23.3	39.3	39.3
H_2 Content (kg)	0.79	2.33	1.96	3.83	0.84	1.52	1.21	4.65
Weight Eff. H_2 Content ($kg.H_2/kg$)	0.044	0.049	0.036	0.041	0.047	0.047	0.047	0.055
Volumetric H_2 Content ($kg.H_2/L^3$)	0.016	0.016	0.025	0.026	0.014	0.015	0.021	0.023
Gravimetric Energy Density (kWh/kg.)	1.467	1.633	1.200	1.367	1.567	1.567	1.567	1.833
Volumetric Energy Density (kWh/L)	0.533	0.533	0.833	0.867	0.467	0.500	0.700	0.767

CHAPTER 3

MECHANICS OF COMPOSITES

3.1. Introduction

The mechanics of materials is based on analytical approaches being the concepts of stress, strains, elastic-plastic deformations and fracture mechanisms to engineering problems which deals with the behavior of material and objects subjected to mechanical and environmental effects such as static and dynamic loads, temperature, moisture and radiation. The analysis includes conventional materials; steel, aluminum, copper, bronze etc. which are are isotropic and homogenous and composite materials such as CFRP, GFRP, plant fiber reinforced plastics etc. which are anisotropic and non-homogeneous. Since the properties of anisotropic materials are dependent on location and orientation, analysis of them requires more effort when compared to analysis of isotropic materials [78].

There are three structural levels of composites which can be mechanically analyzed; basic/elemental level, microstructural level and macrostructural level. In first phase, single molecules and crystal cells are the scope of analysis. In second level, it includes crystals, phases and compound. The interactions of the body parts are microscopic level as being in Nano-meter sized particles. Non-homogenous environment exists. Macrostructural type is the most important for the subject of this study. Since it consists of the mechanics of matrices, particles and fibers. In this level, environment of the composite is assumed as homogenous. The interactions of the components and the effects of these interactions on the overall reactions of the laminate are determined. In order to analyze the overall behavior of the structure as the function of the properties of the laminate and the fiber orientations, the macromechanical analysis is carried out in the form of the lamination theory [79, 82].

3.2. Classical Lamination Theory

In classical lamination theory, each composite layer is assumed as thin, homogenous, linear-elastic, anisotropic and perfectly bonded. It is applied to determine

mechanical behavior of laminated composites. In order to use the theory for laminated composites, there are number of assumptions which must be provided [79].

- The thickness of composite part is much smaller than its edge dimensions. It is uniform and constant. The loadings are only operated on 2D laminated composite and composite is subjected to plane stress. This also applies for thin walled pressure vessels $\left(\sigma_z = \tau_{xz} = \tau_{yz} = 0\right)$.
- For thin- walled composite pressure vessel, this theory is acceptable if the thickness of whole composite part to inner radius of vessel ratio is less than 1/10.
- Displacements through thickness direction are small and continuous along with laminate. ($|u|, |v|, |w| << |h|$, where h is the laminate thickness)
- The plane displacements along x and y directions are linear functions of z axis.
- Since stress distribution are straight and perpendicular to the middle surface so that it maintains its state throughout deformation. Therefore, it is uniform through the wall thickness. ($\gamma_{xz} = \gamma_{yz} = 0$)
- Mechanical analysis considers inner radius of vessel and thickness of the cylinder wall as geometric input while length of the cylinder is not critical.
- Working fluid; hydrogen in this case, has negligible weight [83].

In this thesis, cylindrical Type III pressurized hydrogen composite storage vessels are investigated. Loadings must be defined in cylindrical coordinate system due to the shape of the vessel. Global coordinate of the material is defined in radial (r), hoop (θ) and axis (x) directions and local coordinates with respect to fiber direction is denoted by 1 (fiber direction), 2 (perpendicular to fiber direction) and 3 (perpendicular to both fiber and laminate plane direction). Fiber angle is indicated by θ. n-layered laminated structure with the thickness h is represented as in Figure 3.1. Stacking sequence of laminated composite structure is illustrated in Figure 3.2.

Type III cylindrical storage vessels consist of two differently classified material which must be taken into account during analysis; composite section and liner section. The material of liner is aluminum which is isotropic. Therefore, the only mechanical requirement for liner is reduced stiffness matrix.

$$Q_{liner} = \begin{pmatrix} Q_{11,liner} & Q_{12,liner} & Q_{16,liner} \\ Q_{12,liner} & Q_{22,liner} & Q_{26,liner} \\ Q_{16,liner} & Q_{26,liner} & Q_{66,liner} \end{pmatrix} \tag{3.1}$$

where $Q_{ij,liner}$

$$Q_{11,liner} = \frac{E_{liner}}{1-(v_{21,liner}.v_{12,liner})} \tag{3.2}$$

$$Q_{22,liner} = \frac{E_{liner}}{1-(v_{21,liner}.v_{12,liner})} \tag{3.3}$$

$$Q_{12,liner} = \frac{v_{12,liner}.E_{liner}}{1-v_{21,liner}.v_{12,liner}} \tag{3.4}$$

$$Q_{16,liner} = 0 \tag{3.5}$$

$$Q_{26,liner} = 0 \tag{3.6}$$

$$Q_{66,liner} = G^{ult}_{12,liner} \tag{3.7}$$

Oppositely, laminated carbon fiber reinforced epoxy polymer forms the composite section of the vessels which is anisotropic.

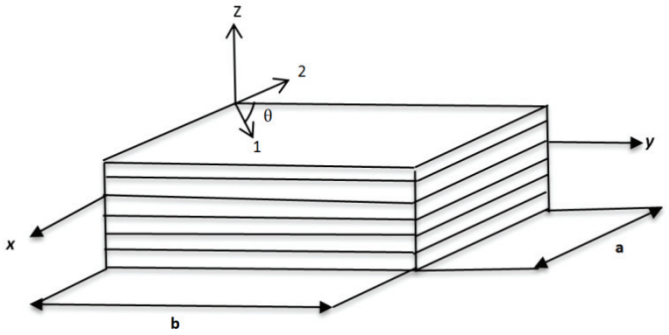

Figure 3.1 Global and local directions of laminated fiber reinforced composite [78]

The strains at any location in laminate with respect to cylindrical coordinates are written in below;

$$\begin{bmatrix} \varepsilon_x \\ \varepsilon_y \\ \gamma_s \end{bmatrix} = \begin{bmatrix} \varepsilon_x^o \\ \varepsilon_y^o \\ \gamma_s \end{bmatrix} + z \begin{bmatrix} \kappa_x \\ \kappa_y \\ \kappa_s \end{bmatrix} \tag{3.8}$$

where [ε^o] are the mid-plane strains and [κ] are curvatures, respectively.

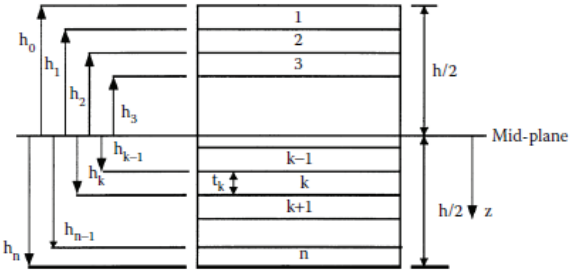

Figure 3.2 Stacking sequence organization of thin fiber reinforced composite [78]

Global stresses and strains for k-th layer are related each other affected by reduced laminate stiffness matrices ([$\overline{Q}_{ij}$]$_k$), curvatures and mid-plane strains.

$$\begin{bmatrix} \sigma_x \\ \sigma_y \\ \sigma_{xy} \end{bmatrix}_k = \begin{bmatrix} \overline{Q}_{11} & \overline{Q}_{12} & \overline{Q}_{16} \\ \overline{Q}_{12} & \overline{Q}_{22} & \overline{Q}_{26} \\ \overline{Q}_{16} & \overline{Q}_{26} & \overline{Q}_{66} \end{bmatrix}_k \left(\begin{bmatrix} \varepsilon_x^o \\ \varepsilon_y^o \\ \varepsilon_{xy}^o \end{bmatrix} + z \begin{bmatrix} \kappa_x \\ \kappa_y \\ \kappa_{xy} \end{bmatrix} \right)_k \tag{3.9}$$

Reduced stiffness for a laminate; [$\overline{Q}_{ij}$] are related with reduced stiffness quantities for the material [Q_{ij}];

$$\overline{Q}_{11} = Q_{11}c^4 + Q_{22}s^4 + 2(Q_{12} + 2Q_{66})s^2c^2 \tag{3.10}$$

$$\overline{Q}_{12} = (Q_{11} + Q_{22} - 4Q_{66})s^2c^2 + Q_{12}(c^4 + s^4) \tag{3.11}$$

$$\overline{Q}_{22} = Q_{11}s^4 + Q_{22}c^4 + 2(Q_{12} + 2Q_{66})s^2c^2 \tag{3.12}$$

$$\overline{Q}_{16} = (Q_{11} - Q_{12} - 2Q_{66})sc^3 - (Q_{22} - Q_{12} - 2Q_{66})s^3c \tag{3.13}$$

$$\overline{Q}_{26} = (Q_{11} - Q_{12} - 2Q_{66})cs^3 - (Q_{22} - Q_{12} - 2Q_{66})sc^3 \tag{3.14}$$

$$\overline{Q}_{66} = (Q_{11} + Q_{22} - 2Q_{12} - 2Q_{66})s^2c^2 + Q_{66}(c^4 + s^4) \tag{3.15}$$

where [Q_{ij}] are

$$Q_{11} = \frac{E_1}{1 - \nu_{21}\nu_{12}} \tag{3.16}$$

$$Q_{12} = \frac{\nu_{12}E_2}{1 - \nu_{21}\nu_{12}} \tag{3.17}$$

$$Q_{22} = \frac{E_2}{1 - \nu_{21}\nu_{12}} \tag{3.18}$$

$$Q_{66} = G_{12} \tag{3.19}$$

Resultant loads and moments for a lamina are observed in principal and transverse directions as shown in Figure 3.3.

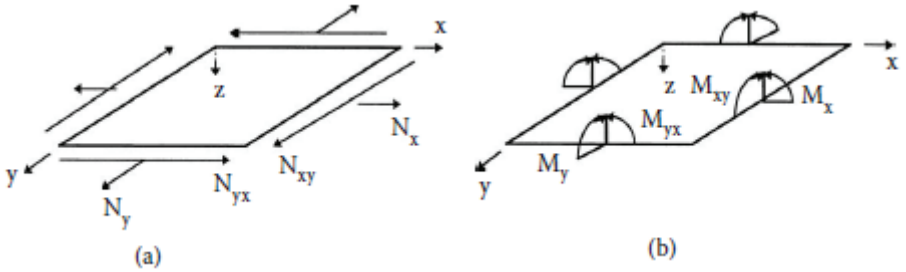

Figure 3.3 Illustration of resultant loads and moments on laminates [39]

The relationship of applied normal load resultants; N_x, N_y and shear load resultant; N_{xy} (stress per unit thickness), moment couple resultants; M_x, M_y and M_{xy} for laminated composite structure is given below;

$$\begin{bmatrix} N_x \\ N_y \\ N_{xy} \end{bmatrix} = \begin{bmatrix} A_{11} & A_{12} & A_{16} \\ A_{12} & A_{22} & A_{26} \\ A_{16} & A_{26} & A_{66} \end{bmatrix} \begin{bmatrix} \varepsilon_x^0 \\ \varepsilon_y^0 \\ \gamma_{xy}^0 \end{bmatrix} + \begin{bmatrix} B_{11} & B_{12} & B_{16} \\ B_{12} & B_{22} & B_{26} \\ B_{16} & B_{26} & B_{66} \end{bmatrix} \begin{bmatrix} \kappa_x \\ \kappa_y \\ \kappa_{xy} \end{bmatrix} \tag{3.20}$$

$$\begin{bmatrix} M_x \\ M_y \\ M_{xy} \end{bmatrix} = \begin{bmatrix} B_{11} & B_{12} & B_{16} \\ B_{12} & B_{22} & B_{26} \\ B_{16} & B_{26} & B_{66} \end{bmatrix} \begin{bmatrix} \varepsilon_x^0 \\ \varepsilon_y^0 \\ \gamma_{xy}^0 \end{bmatrix} + \begin{bmatrix} D_{11} & D_{12} & D_{16} \\ D_{12} & D_{22} & D_{26} \\ D_{16} & D_{26} & D_{66} \end{bmatrix} \begin{bmatrix} \kappa_x \\ \kappa_y \\ \kappa_{xy} \end{bmatrix} \tag{3.21}$$

where [A], [B] and [D] matrices are expressed in Equation 3.22, Equation 3.23 and Equation 3.24.

$$A_{ij} = \sum_{k=1}^{n} [(\overline{Q}_{ij})]_k (h_k - h_{k-1}) + Q_{liner}.h_{liner} \qquad i,j = 1,2,6 \qquad (3.22)$$

$$B_{ij} = \frac{1}{2}\sum_{k=1}^{n} [(\overline{Q}_{ij})]_k (h_k^2 - h_{k-1}^2) + Q_{liner}.h_{liner} \qquad i,j = 1,2,6 \qquad (3.23)$$

$$D_{ij} = \frac{1}{3}\sum_{k=1}^{n} [(\overline{Q}_{ij})]_k (h_k^3 - h_{k-1}^3) + Q_{liner}.h_{liner} \qquad i,j = 1,2,6 \qquad (3.24)$$

where h_{liner} is the liner thickness, Extensional stiffness matrix, [A]; regards in plane forces to the in-plane strains, stretching-coupling matrix, [B]; regards for forces and mid-plane strains, moments and mid-plane curvatures and flexural rigidity matrix, [D]; regards moments and curvatures [39].

Since symmetry between layers and geometry exist, [B] matrix becomes zero. Moreover, the only loading is internal pressure, therefore there are no moment resultants in problem designs, so [D] matrix is also zero. From Equations 3.20 and 3.21, the relation between load resultants and strains are determined as Equation 3.25.

$$\begin{bmatrix} N_x \\ N_y \\ N_{xy} \\ M_x \\ M_y \\ M_{xy} \end{bmatrix} = \begin{bmatrix} A_{11} & A_{12} & A_{16} & B_{11} & B_{12} & B_{16} \\ A_{12} & A_{22} & A_{26} & B_{12} & B_{22} & B_{26} \\ A_{16} & A_{26} & A_{66} & B_{16} & B_{26} & B_{66} \\ B_{11} & B_{12} & B_{16} & D_{11} & D_{12} & D_{16} \\ B_{12} & B_{22} & B_{26} & D_{12} & D_{22} & D_{26} \\ B_{16} & B_{26} & B_{66} & D_{16} & D_{26} & D_{66} \end{bmatrix} \begin{bmatrix} \varepsilon_x^0 \\ \varepsilon_y^0 \\ \gamma_{xy}^0 \\ \kappa_x \\ \kappa_y \\ \kappa_{xy} \end{bmatrix}$$

$$\downarrow$$

$$\begin{bmatrix} N_x \\ N_y \\ N_{xy} \end{bmatrix} = \begin{bmatrix} A_{11} & A_{12} & A_{16} \\ A_{12} & A_{22} & A_{26} \\ A_{16} & A_{26} & A_{66} \end{bmatrix} \begin{bmatrix} \varepsilon_x^0 \\ \varepsilon_y^0 \\ \gamma_{xy}^0 \end{bmatrix} \qquad (3.25)$$

To determine midplane strains, each side of Equation 3.25 is multiplied with inverse of [A] matrix;

$$\begin{bmatrix} \varepsilon_x^0 \\ \varepsilon_y^0 \\ \gamma_{xy}^0 \end{bmatrix} = \begin{bmatrix} A_{11} & A_{12} & A_{16} \\ A_{12} & A_{22} & A_{26} \\ A_{16} & A_{26} & A_{66} \end{bmatrix}^{-1} \begin{bmatrix} N_x \\ N_y \\ N_{xy} \end{bmatrix} \tag{3.26}$$

Since curvatures don't exist due to symmetry and loading type, Equation 3.8 is substituted this;

$$\begin{bmatrix} \varepsilon_x \\ \varepsilon_y \\ \gamma_{xy} \end{bmatrix} = \begin{bmatrix} \varepsilon_x^0 \\ \varepsilon_y^0 \\ \gamma_{xy}^0 \end{bmatrix} \tag{3.27}$$

From Equations 3.26 and 3.27, global strain matrix is determined;

$$\begin{bmatrix} \varepsilon_x \\ \varepsilon_y \\ \gamma_{xy} \end{bmatrix} = \begin{bmatrix} A_{11} & A_{12} & A_{16} \\ A_{12} & A_{22} & A_{26} \\ A_{16} & A_{26} & A_{66} \end{bmatrix}^{-1} \begin{bmatrix} N_x \\ N_y \\ N_{xy} \end{bmatrix} \tag{3.28}$$

Equation 3.9 is substituted to Equation 3.29;

$$\begin{bmatrix} \sigma_x \\ \sigma_y \\ \sigma_{xy} \end{bmatrix}_k = \begin{bmatrix} \overline{Q}_{11} & \overline{Q}_{12} & \overline{Q}_{16} \\ \overline{Q}_{12} & \overline{Q}_{22} & \overline{Q}_{26} \\ \overline{Q}_{16} & \overline{Q}_{26} & \overline{Q}_{66} \end{bmatrix}_k \begin{bmatrix} \varepsilon_x \\ \varepsilon_y \\ \gamma_{xy} \end{bmatrix}_k \tag{3.29}$$

In conclusion, local strains and stress can be expressed from global stress and strains;

$$\begin{bmatrix} \varepsilon_1 \\ \varepsilon_2 \\ \varepsilon_{12} \end{bmatrix} = [R][T][R]^{-1} \begin{bmatrix} \varepsilon_x \\ \varepsilon_y \\ \varepsilon_{xy} \end{bmatrix} \tag{3.30}$$

$$\begin{bmatrix} \sigma_1 \\ \sigma_2 \\ \sigma_{12} \end{bmatrix} = [T] \begin{bmatrix} \sigma_x \\ \sigma_y \\ \sigma_{xy} \end{bmatrix} \tag{3.31}$$

where

$$[R] = \begin{bmatrix} 1 & 0 & 0 \\ 0 & 1 & 0 \\ 0 & 0 & 2 \end{bmatrix} \tag{3.32}$$

and $[T]$ is the transformation matrix which provides a relationship between stress-strains in global coordinates to stress-strains in local coordinates by cutting at an angle θ normal to 1 (fiber direction) [39]

$$[T]=\begin{bmatrix} \cos^2\theta & \sin^2\theta & 2\sin\theta\cos\theta \\ \sin^2\theta & \cos^2\theta & -2\sin\theta\cos\theta \\ -\sin\theta\cos\theta & \sin\theta\cos\theta & \cos^2\theta-\sin^2\theta \end{bmatrix} \quad (3.33)$$

3.3. Stress Analysis of Thin-Walled Pressure Vessels

Pressurized gas thin-walled vessels are subjected to inner pressure, P. This pressure causes load resultants in hoop (circumferential) and axial direction; N_θ and N_x. Therefore, principal stresses at hoop and axial directions occured. No shear stresses form on these faces due to symmetry of the vessel and its loading, P. Hence, forming stresses; σ_θ and σ_x are the principal stresses. σ_θ is called hoop (circumferential) stress and σ_x is axial (longitudinal) stress because of their directions as shown in Figure 3.3a [84]. It should be noted that the notations of load or stress or strain resultants might be used differently in literature. In previous section, N_y is hoop load (N_θ) and N_{xy} is transverse load resultant ($N_{x\theta}$).

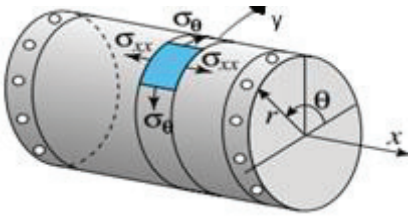

Figure 3.3 Hoop and axial stresses forming due to the internal pressure [84]

In order to define hoop and axial stresses, free body diagrams are set. As shown in Figure 3.3.b, two cuts are made; mn and pq. The cuts include half of the vessel and fluid included in the vessel which causes inner pressure. Hoop stress; σ_θ and internal pressure; P, act on the longitudinal cut being "plane mpqn" and axial stress; σ_x and P, act on each faces of the free body. It should be noted that the weight of the tank and its content are disregarded.

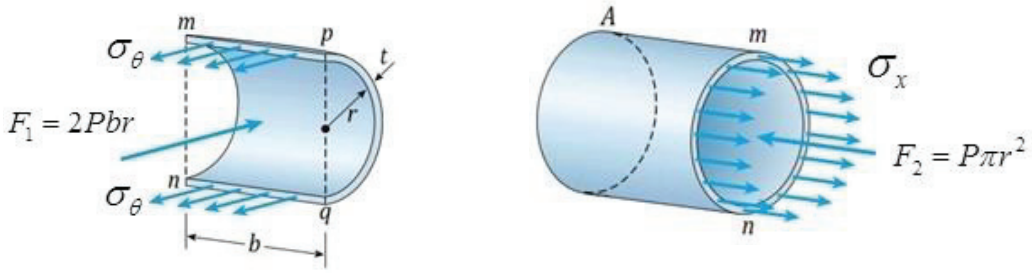

Figure 3.4 Determining of hoop and axial stress in a pressure vessel [84]

Resultant force formed by hoop stress and pressure equal $\sigma_\theta(2bt)$ and $2Pbr$ where r is the inner radius of the cylindrical pressure vessel. From resultant force equilibrium, hoop stress is determined from the force equilibrium at Equation 3.34 and it is given in Equation 3.35. Load resultant at hoop direction is given at Equation 3.36.

$$\sigma_\theta(2bt) - 2Pbr = 0 \tag{3.34}$$

$$\sigma_\theta = \frac{Pr}{t} \tag{3.35}$$

$$N_\theta = Pr \tag{3.36}$$

Since pressure vessel is thin walled, the stress obtained through wall thickness is uniformly distributed.

The axial stress; σ_x, is determined from the force resultant equilibrium of a free body of the part of the vessel of cross section; mn. The resultant force due to axial stress is $\sigma_x(2\pi rt)$ and other force resultant is observed due to inner pressure as $P\pi r^2$. The equilibrium of resultant forces and axial stress are given in Equation 3.37 and Equation 3.38. Load resultant at axial direction is given at Equation 3.39.

$$\sigma_x(2\pi rt) - P\pi r^2 = 0 \tag{3.37}$$

$$\sigma_x = \frac{Pr}{2t} \tag{3.38}$$

$$N_x = \frac{Pr}{2} \tag{3.39}$$

As seen from Equation 3.35 and Equation 3.38, hoop stress is equal to twice the axial stress. This result shows that engineer should strengthen the parts in hoop direction at least twice times than the parts in axial direction [84].

In Mathematica code, load resultants in hoop and axial directions (Equations 3.36 and 3.39) are used to determine local stress and strains.

3.4. Failure Theories for a Composite Lamina

Efficient and safe use of materials for an application is the significant indicator of a successful design. Therefore, failure theories are developed to predict state of stress and material failures. They are used whether a material is mathematically failed or not under loadings and their validations are based on experiments. For example, while maximum stress failure theory can suggest accurate results for failures of isotropic materials, Tsai-Wu failure theory might be more convenient to predict failure of anisotropic materials according to validations from experiments. There are two different approaches to failure of materials; non-interactive criteria and interactive criteria [39].

The theories categorized as non-interactive doesn't include the interactions between stress or strain components while predicting the failure of material. The stress or strain accumulated in the structure is compared with the strength of it to determine whether material is failed or safe. Maximum Stress and Maximum Strain theories are common failure criteria classified as non-interactive [80].

An interactive criterion predicts material failure based on the interaction of stress components or strain components built on the structure. There are three types of interactive criteria; polynomial theories, direct mode determining theories and strain energy theories. Polynomial Theories include Tsai-Wu theory and Tsai-Hill theory while Hashin's Criterion and Hashin-Rotem failure theory, Eckold's Criteria, Edge's Criteria, Hart-Smith's Criteria, Puck's Criteria, Sun's Criteria, Wolfe's Criteria and Zinoviev Criteria are classified as direct mode determining theories [80].

In this study, an interactive polynomial criterion; Tsai-Wu Failure Theory, a non-interactive criterion; Maximum Stress failure theory and a direct mode determining theory; Hashin-Rotem criteria are used for stress analysis and burst pressure of the composite vessels. Main aim for using differently classified failure theories is to reveal

their differences according to optimum stacking sequence, number of plies and CPU time.

3.4.1. Maximum Stress Criterion

According to this theory, laminated composite is failed, if one of the conditions below is not ensured;

$$-(\sigma_1^C)_{ult} < \sigma_1 < (\sigma_1^T)_{ult} \text{ , or} \tag{3.40}$$

$$-(\sigma_2^C)_{ult} < \sigma_2 < (\sigma_2^T)_{ult} \text{ , or} \tag{3.41}$$

$$-(\tau_{12})_{ult} < \tau_{12} < (\tau_{12})_{ult} \tag{3.42}$$

Therefore, according to this theory, failure of material is observed when at least one stress component through one of the local direction exceeds the corresponding strength component in same direction. However, this theory might not give applicable results for failure of brittle materials having longitudinal and transverse tension. It doesn't include uniaxial interactions (stress interaction), so that it considers with less accuracy when multiaxial stress combination is present [39].

3.4.2 Tsai-Wu Failure Criterion

Anisotropic nature of composites requires different failure theory approaches. Tsai-Wu failure criterion which is derived from Von Mises Yield Criterion and based on the total stain energy failure theory of Beltrami is one of the most common failure theories to predict failure of a composite lamina in plane stress. A composite lamina is assumed to be failed, if the condition given in below is not provided [78]

$$F_{11}\sigma_1^2 + F_1\sigma_1 + F_2\sigma_2 + 2F_{12}\sigma_1\sigma_2 + F_{22}\sigma_2^2 + F_{21}\tau_{12}^2 < 1 \tag{3.43}$$

where F_{ij} are defined as strength components of the material

$$F_1 = \frac{1}{X_T} - \frac{1}{X_C}, \qquad F_2 = \frac{1}{Y_T} - \frac{1}{Y_C}$$

$$F_{11} = \frac{1}{X_T X_C}, \qquad F_{22} = \frac{1}{Y_T Y_C}, \qquad F_{12} \cong -\frac{1}{2}\sqrt{F_{11}F_{22}} \tag{3.44}$$

X_T: Tensile strength in fiber direction

X_C: Compressive strength in fiber direction

Y_T: Tensile strength in transverse of fiber direction

Y_C: Compressive strength in transverse of fiber direction

This theory provides two significant advantages such that stress components on the structure are in interaction each other and it seperates the strength components as tension and compression. On the other hand, the determination of the strength component; F_{12}, might not be accurate [81].

3.4.3. Hashin-Rotem Criterion

This failure theory is related to fiber and matrix failures and it consist of four failure modes being tensile fiber failure, compressive fiber failure, tensile matrix failure, compressive matrix failure. If one of the conditions below is violated, material is assumed to be failed [60].

Fiber failure in tension ($\sigma_1>0$)

$$\sigma_1=(\sigma_1^T)_{ult} \tag{3.45}$$

Fiber failure in compression ($\sigma_1<0$)

$$-\sigma_1=(\sigma_1^C)_{ult} \tag{3.46}$$

Matrix failure in tension ($\sigma_2>0$)

$$\left(\frac{\sigma_2}{(\sigma_2^T)_{ult}}\right)^2+\left(\frac{\tau_{12}}{(\tau_{12})_{ult}}\right)^2=1 \tag{3.47}$$

Matrix failure in compression ($\sigma_2<0$)

$$\left(\frac{\sigma_2}{(\sigma_2^C)_{ult}}\right)^2+\left(\frac{\tau_{12}}{(\tau_{12})_{ult}}\right)^2=1 \tag{3.48}$$

CHAPTER 4

OPTIMIZATION

4.1. Introduction

Optimization is a series of mathematical process aiming to find optimum design for a case by minimization or maximization of defined single or multi objectives with satisfying of given constraints. Optimization is frequently addressed for the engineering problems being failure, weight, cost, temperature, buckling, vibration etc. In these problems, minimization or maximization of objective or multi-objectives are applied to obtain optimum solutions. In first type of optimization, there is only one function to be minimized or maximized with single or more constraints and relations. In some cases, optimizing of only one objective might conflict with other parameters. Therefore, optimization problems having multi bounds should be optimized considering multi-objective design [85]. Since it isn't possible to obtain the best solutions for each objective, Pareto optimal solutions are determined using the multi-objective approach. In this case, only one solution is picked among the solution pool to use for engineering problem [25].

Laminated composite structures are anisotropic materials making them more complicated and difficult to design analytically because of consisting highly nonlinear functions. In this case, traditional optimization approaches might be insufficient from the specifications which optimization of these materials might require. Hence, stochastic search algorithms are more suitable for the optimization problems of composites. Differential Evolution (DE), Nelder Mead (NM), Genetic Algorithm (GA), Simulated Annealing (SA), Random Search (RS) are frequently used stochastic optimization algorithms.

In this study, the design and optimization of pressurized hydrogen composite storage vessels are performed by using MATHEMATICA software which offers appropriate platform for the optimization problems [95]. Program consists of four stochastic optimization algorithms in its database being DE, NM, RS and SA which are extensively used by researchers in the design and optimization cases of composites. Problems included in the study are solved by using DE and NM. By this way,

comparison of two different stochastic approaches is examined. In these problems, main objective is to minimize failure criteria index by finding optimum stacking sequence and number of plies of laminated composite part of the vessels (Tsai-Wu, Maximum Stress and Hashin-Rotem) with maintaining the constraints. Optimization performed in the study can be called as single objective.

4.2. Single Objective Optimization

An objective function, design parameters, constraints and relations of constraints are included in single objective optimization. This optimization procedure can be examined as below.

Minimize: $f(x_1, x_2, ..., x_n)$

Constraint: $h_i(x_1, x_2, ..., x_n) = 0 \qquad i = 1, 2, ...r$

$g_j(x_1, x_2, ..., x_n) = 0 \qquad j = 1, 2, ...m$

$x^L \leq x_1, x_2, ..., x_n \leq x^U$

where f is the objective function, x_1, x_2,…,x_n being design variables, h and g are the constraints of the problem while x^L and x^U define the lower and upper bonds. As mentioned previously, stiffness, strength, fatigue failure, mass, displacements, thickness, buckling loads, cost, weight and natural frequency can be utilized as objective functions of a problem [86]

4.3. Multi Objective Optimization

Multi objective optimization which includes multiple objective functions is expressed as following;

Minimize: $f_1(x_1, x_2, ..., x_n), f_2(x_1, x_2, ..., x_n), \ldots, f_s(x_1, x_2, ..., x_n)$

Constraint: $h_i(x_1, x_2, ..., x_n) = 0 \qquad i = 1, 2, ...r$

$$g_j(x_1, x_2, ..., x_n) = 0 \qquad j = 1, 2, ...m$$

$$x^L \leq x_1, x_2, ..., x_n \leq x^U$$

Here, $f_1, f_2, ..., f_s$ indicate the objective functions to be maximized or minimized. As oppose the traditional optimization approaches, an error function can be defined into objectives. The advantage of error function formulation in multi objective optimization is to turn constrained optimization problems into the unconstrained ones which enable it to be applied to the problem by any of the unconstrained methods [87]. In the study, error function can be thought as the minimum number of laminated composite plies which satisfy optimum stacking sequence at desired burst pressure. Hence, code minimizes the failure index with respect to first-ply failure (objective function) by obtaining optimum stacking sequence formation at burst pressure with a minimum number of plies.

4.4. Stochastic Search Algorithms

In general, optimization approaches are divided in the two main categories as traditional and non-traditional. Constrained Variation and Lagrange Multipliers being analytical traditional methods are specialized to obtain the optimum solution of only continuous and differentiable functions. Since, problems of composite structures consist of highly discrete search spaces, traditional optimization methods fail to meet obtaining optimum results. In these situations, non-traditional search algorithms such as DE, NM, SA, and GA are preferred to find optimum solutions. Rao (2009) [87] expressed a detailed discussion of different optimization methods for general applications while Gurdal et al. (1999) [86], studied them for the usage in composites. In this study, DE and NM are used to obtain optimum stacking sequence design at desired burst pressure of composite pressure vessels. In following sections, procedures for these algorithms are explained in step wise formation.

4.4.1. Differential Evolution Algorithm (DE)

Differential Evolution is one of the derivation based stochastic search algorithm which is capable to obtain alternative solutions for some complicated composite design and optimization problems. As shown in Figure 4.1, it consists of four main stages

which are initialization, mutation, crossover and selection. Scaling factor, crossover and population size are critical parameters in the event of finding optimum results. In process, DE doesn't consider a single solution but oppositely includes a population of solutions in iterations which results being a computationally expensive optimization algorithm. On the other hand, this feature makes DE efficient and stable in obtaining global optimum of the objective functions while finding the global optima isn't certain [88].

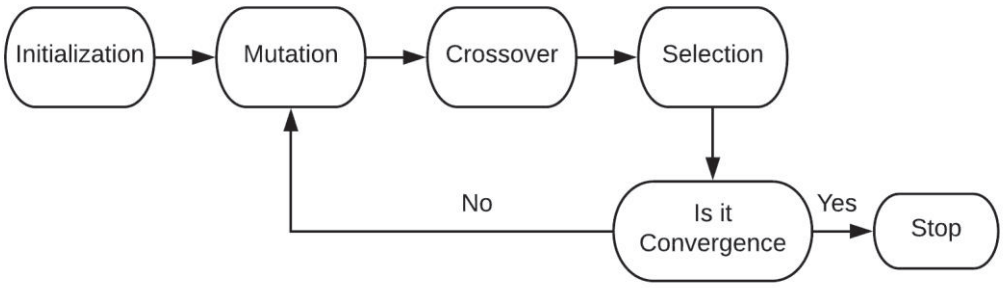

Figure 4.1 Flowchart of Differential Evolution algorithm (Adapted from [93])

There are a number of approaches to populate initialization process which is the first step of DE. One of the most widely used approaches is random generation. Here, a population of n points; $\{x_1, x_2,...,x_k,\ldots,x_r\}$ are maintained where generally r is larger than k which defines the number of variables. In Mutation step, the variation of the genetics from one generation of a population to the next generation is controlled by a genetic operator. Therefore, the solution obtained during this step is different that it generally provides better solution. Crossover which is the third step of the algorithm is responsible to obtain populations having more variety. The work scheme of this step is set by the inspiration of genetic diversity of living things. The interchange of genetic material between chromosomes encourages the genetic diversity. Then, distinction of the gene strings of the chromosomes is actualized at the same point in female and male which result born of the child. In last step, selection of populations is made. By this way, the new individual is brought in the new population [86, 89, 90]

4.4.2. Nelder-Mead Algorithm (NM)

Also, known as Simplex Search, Nelder Mead algorithm is one of the derivative free optimization methods among other traditional local search algorithms. It was firstly

designed for unconstrained optimization problem [91]. Nelder Mead is not a global optimization algorithm. Hence, it is not an ideal search method for optimization problems having many local minima. However, it proves its efficiency for problems having small number of local minima. As DE, NM has also similar steps which adjust the performance of the algorithm. These steps are reflection, expansion, contraction and shrinkage. When compared to DE, NM has more capability to produce considerable improvements just in few iterations. Being one of the marked properties of NM, this delivers quite adequate results in less time. In addition to this, except of shrink transformations, algorithm only requires one or two function evaluations in each iteration which is rarely seen in practice for an optimization algorithm. Since, each function evolution for a certain application results cost increment or consuming of time. Therefore, NM is frequently preferred in optimization problems of engineering applications having not much local minima. Moreover, NM has the required flexibility to explore challenging domains since its simplex can change its orientation, size and shape to adapt more in local contour of the objective function [92]. The adjustable parameters of DE and NM algorithms are listed in Table 4.1 below.

Table 4.1 Adjustable properties of DE and NM [95]

Adjustable Parameters	**DE**	**NM**
Cross Probability	0.5	-
Random Seed	0	0
Scaling Factor	0.6	-
Search Points	-	-
Tolerance	0.001	0.001
Contract Ratio	-	0.5
Expand Ratio	-	2.0
Reflect Ratio	-	1.0
Shrink Ratio	-	0.5
Level Iterations	-	-
Perturbation Scale	-	-

Process flowchart of the algorithm is shown in Figure 4.2.

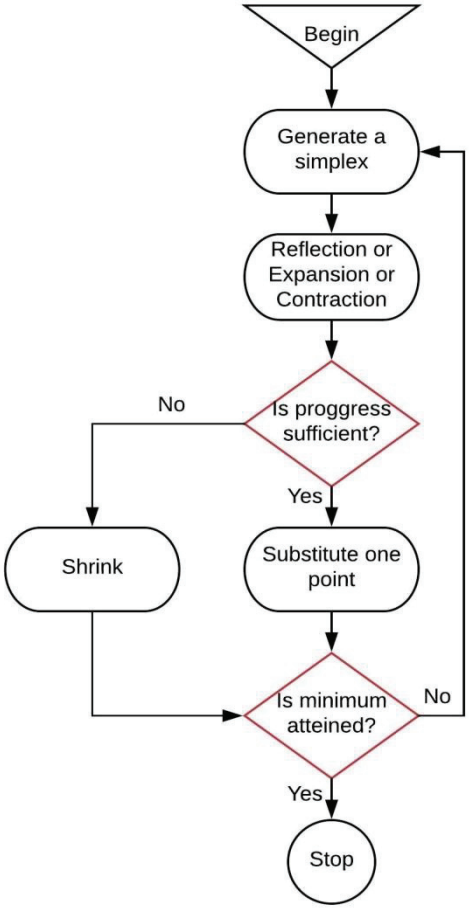

Figure 4.2 Flowchart of the NM algorithm. (Adapted from [94])

CHAPTER 5

RESULTS AND DISCUSSION

5.1. Problem Statement

Determination of the optimum stacking sequence design of composite pressure storage vessel is critical because the vessels containing any pressurized gas must satisfy strength requirements and safety factor to meet strict regulations and standards of application areas such as hydrogen fuel cell vehicles. Some benefits of optimization process are preventing excessive material usage, time, and decreasing the cost of design and manufacturing processes. Therefore, researchers studying on maximization of strength of pressure vessels generally focus on the optimization of stacking sequence at working pressure, proof pressure (safety factor of 1.5) or burst pressure (safety factor of 2.0 or higher). By doing this, designs can meet standards in safety margin.

In this chapter, stacking sequence optimization of filament wound composite pressure vessels with metal liner (Type III) have been solved by using stochastic search algorithms. Stress and strain analyses are determined using classical lamination theory incorporating with first-ply failure approach. Accordingly, four different composite pressure vessel designs which have different storage volume, identical working pressure of 700-bar and safety factor of 2.0 have been investigated. Main objective is the optimization of stacking sequences of the considered designs at burst pressure. Therefore, each optimized design must resist failure until the burst pressure of 1400 bar. Moreover, the effect of volume differences on the stacking sequence designs has been investigated. The parameters used in calculations such as internal pressure P = 1400 bar, inner radius R, cylindrical coordinates, fiber orientation angle θ and boundary conditions are shown in Figure 5.1. The geometrical properties of the design problems are also presented in Table 5.1.

First-ply failure of designs has been predicted using Tsai-Wu, Hashin-Rotem and Maximum Stress failure theories. Optimum stacking sequences have been obtained using stochastic search algorithms, Differential Evolution and Nelder-Mead. Composite part of the vessels is carbon fiber reinforced epoxy polymer and liner material is aluminum 6061-T6 alloy.

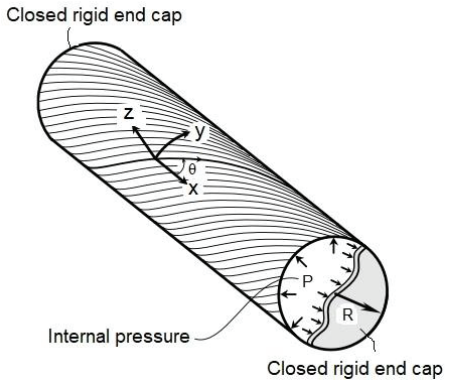

Figure 5.1 Illustration for loading type, reference coordinate system and boundary condition of the considered designs [25]

Table 5.1 Geometrical properties of the design problems

Properties / Designs	Volume (lt)	Inner Radius (mm)	Thickness of a ply (mm)	Thickness of liner (mm)	Length (mm)
Design I	5	56.42	0.127	3	500
Design II	10	79.79			
Design III	20	112.94			
Design IV	50	178.4			

The elastic properties are taken from the previous study [35] and given in Table 5.7. Fiber orientation angles and number of layers have been taken as design variable. Fiber orientation angles are considered as continuous in the optimization process $(-90 \le \theta \le 90)$. According to CLT, the ratio of total wall thickness to inner radius must not exceed 1/10. In this manner, obtained number of layers must not exceed 20 layers for Design I, 39 layers for Design II, 65 layers for Design III and 116 layers for Design IV.

The mathematical representation of the optimization problem for this study can be stated as follows:

Find: $\{\theta_p, n\}, \theta_p \in [\theta_1, -\theta_1, \dots, \theta_n, -\theta_n]_s, \theta_p \in$ Integers, where

number of layers for;

Design I ≤ 20,

Design II ≤ 39,

Design III ≤ 65,

Design IV ≤ 116

Minimize: Tsai-Wu, Hashin-Rotem and Maximum Stress failure index

Constraints: Tsai-Wu≤ 1, Hashin-Rotem ≤ 1,

Maximum stress ≤ 1 (for each ply)

$-90 \leq \theta_p \leq 90$

Symmetry

Methods: Differential Evolution and Nelder -Mead (applied separately)

Iteration has been set to 500

In optimization process, solutions which don't include balance in fiber orientation are also involved such as $[\pm\theta_1/\pm\theta_2/.../\pm\theta_{n-1}/\theta_n]_S$ or $[\pm\theta_1/\pm\theta_2/.../\pm\theta_{n-1}/-\theta_n]_S$.

5.2. The Verification of the Developed Code

The verification of the developed code is carried out by the studies from literature considering certain properties in their design cases such as burst pressure, fiber orientation angle, number of layers, inner radius of the cylindrical vessel, thickness of liner, thickness of a ply, ultimate strengths of composite, elastic properties of composite and liner.

Verification 1

First verification of the developed code has been performed from literature [25]. Mechanical properties used have been given in Table 5.2. In their study, pressure vessels have not included liner.

Table 5.2 Mechanical properties [25]

Material	Mechanical Properties									
Carbon fiber/epoxy composite	E_1 (GPa)	E_2 (GPa)	G_{12} (GPa)	ν_{12}	ν_{21}	$\sigma^{ult}_{1,T}$ (MPa)	$\sigma^{ult}_{1,C}$ (MPa)	$\sigma^{ult}_{2,T}$ (MPa)	$\sigma^{ult}_{2,C}$ (MPa)	τ^{ult}_{12} (MPa)
	165.86	9.796	4.96	0.275	0.018	1811.25	1064.35	94.06	220.07	80.68

Design problems are precisely verified and listed in Table 5.3. In this study, determination of the lamina stresses for thin laminates under load resultants was performed using CLT and first-ply failure approach by Tsai-Wu failure theory.

Table 5.3 Validation of the developed code [25]

Design	Fiber Orientation	$P_{failure}$ (MPa) (Tsai-Wu) (CLT)	$P_{failure}$ (MPa) (Tsai-Wu) (Present)
a	$[90]_s$	0.754	**0.7544**
b	$[90/-75/60/90]_s$	0.954	**0.954566**
c	$[0/90_3]_s$	3.512	**3.51275**
d	$[45/-60/60/-60]_s$	3.831	**3.83167**
e	$[90_3/15/-30/90]_s$	5.208	**5.20814**
f	$[90_{10}]_s$	1.886	**1.88608**
g	$[0/75/90_3/-45/90_3]_s$	5.598	**5.59817**
h	$[90_4/0/90_3/0]_s$	7.433	**7.43345**
i	$[90/30/90/-30/15/90_3/-15/90]_s$	9.597	**9.59726**
j	$[90_5/0/90_2/0_2]_s$	9.476	**9.47640**

Verification 2

The other study is used for second verification of the code [20]. The mechanical properties used are given in Table 5.4. Here, pressure vessel without liner was considered.

Table 5.4 Mechanical properties [20]

Material	Mechanical Properties									
Graphite/Epoxy Prepreg	E_1 (GPa)	E_2 (GPa)	G_{12} (GPa)	ν_{12}	ν_{21}	$\sigma^{ult}_{1,T}$ (MPa)	$\sigma^{ult}_{1,C}$ (MPa)	$\sigma^{ult}_{2,T}$ (MPa)	$\sigma^{ult}_{2,C}$ (MPa)	τ^{ult}_{12} (MPa)
	142.5	9.79	4.72	0.27	0.018	2193	2457	41.3	206.8	61.28

It can be seen from the table that the solution obtained by the developed code verifies the burst pressure results. The comparison of the obtained results is given in Table 5.5.

Table 5.5 Verification of the code [20]

Fiber orientation	**$P_{failure}$ (MPa) (Hoffman, Tsai-Hill, Tsai-Wu, Maximum Strain) (Numerical)**	**$P_{failure}$ (MPa) (Experimental)**	**$P_{failure}$ (MPa) (Tsai-Wu) (Present)**
$[\pm 54_2]_S$	5.26	5.39	5.49
$[\pm 54_3]_S$	7.28	7.6	8.24
$[\pm 54_4]_S$	9.22	9.61	10.97

Verification 3

The other study from the literature is used for third verification [28]. Mechanical properties used are presented in Table 5.6.

Table 5.6 Mechanical properties [28]

Material	**Mechanical Properties**									
	E_1 (GPa)	**E_2 (GPa)**	**G_{12} (GPa)**	**ν_{12}**	**ν_{21}**	**$\sigma^{ult}_{1,T}$ (MPa)**	**$\sigma^{ult}_{1,C}$ (MPa)**	**$\sigma^{ult}_{2,T}$ (MPa)**	**$\sigma^{ult}_{2,C}$ (MPa)**	**τ^{ult}_{12} (MPa)**
T700/Epoxy	181	10.3	5.17	0.28	0.016	2150	2150	298	298	778
6061-T6 Al Liner	70	70	26.92	0.3		-				

In their study, authors considered Type III pressure vessel subjected to internal pressure and thermal residual stress. Elastic stress analysis of composite laminates has been performed by using CLT and these calculations have been utilized with the elasto-plastic stress analysis of the liner employing the power hardening theory and Hencky Equation. The damage evolution and the burst failure of the composite laminates have been determined with a developed universal algorithm based on the Hashin last-ply

failure criterion. It can be seen from Table 5.7, obtained burst pressure by the developed code approximates the results of this study. Burst pressure value have been obtained as 147 MPa for Hashin-Rotem, Maximum Strain, Maximum Stress and Tsai-Hill. Discrepancy might have been occurred due to assumption of liner material.

Table 5.7 Verification of developed code using the study [28]

Fiber orientation	**$P_{failure}$ (MPa) (Hashin) (Tsai-Wu) (Analytical)**	**$P_{failure}$ (MPa) (Experimental)**	**$P_{failure}$ (MPa) (Hashin-Rotem, Maximum Strain, Maximum Stress, Tsai Hill) (Present)**
$[\pm 90/\pm 18.9/\pm 90/\pm 28.6/\pm 90]$	135	125	147

Verification 4

Another study of the same research group is used for fourth verification [30]. Material properties are listed in Table 5.8.

Table 5.8 Mechanical properties [30]

Material	**Mechanical Properties**									
	E_1 (GPa)	**E_2 (GPa)**	**G_{12} (GPa)**	**ν_{12}**	**ν_{21}**	**$\sigma^{ult}_{1,T}$ (MPa)**	**$\sigma^{ult}_{1,C}$ (MPa)**	**$\sigma^{ult}_{2,T}$ (MPa)**	**$\sigma^{ult}_{2,C}$ (MPa)**	**τ^{ult}_{12} (MPa)**
T700/Epoxy composite	154.1	10.3	5.17	0.28	0.016	2500	1250	60	186	85
6061-T6 Al Liner	70	70	26.92	0.33		-				

Numerical results for cylindrical pressure vessel design were predicted by using explicit FEA incorporating with Hashin damage initiation criterion. Verification of the developed code for using the study is given in Table 5.9.

Table 5.9 Verification of developed code [30]

Fiber orientation	$P_{failure}$ (MPa) (Hashin failure) (Numerical)	$P_{failure}$ (MPa) (Experimental)	$P_{failure}$ (MPa) (Tsai-Wu) (present)	$P_{failure}$ (MPa) (Maximum-Stress) (present)	$P_{failure}$ (MPa) (Hashin-Rotem) (present)
$[90_2 / \pm 18.9 / 90_2 / \pm 28.9 / 90_2]$	99.8	106	90.4	70	70

Verification 5

Fifth verification of the developed code is performed by using another study from literature [35]. They have considered both Type III and Type IV pressure vessel. Mechanical properties of the design are shown in Table 5.10.

Table 5.10 Mechanical properties [35]

Material	Mechanical Properties									
	E_1 (GPa)	E_2 (GPa)	G_{12} (GPa)	ν_{12}	ν_{21}	$\sigma^{ult}_{1,T}$ (MPa)	$\sigma^{ult}_{1,C}$ (MPa)	$\sigma^{ult}_{2,T}$ (MPa)	$\sigma^{ult}_{2,C}$ (MPa)	τ^{ult}_{12} (MPa)
T700/Epoxy composite	181	10.3	5.86	0.28	0.016	2150	2150	298	298	778
6061 Al Liner	70	70	26.92	0.3		-				

In this study, the failure analysis of optimized pressure vessel design by using Simulated Annealing algorithm has been performed by employing finite element analysis. The plastic behavior of liner was assumed. It can be seen from the Table 5.11, result obtained by the developed code verifies the result of the previous study.

Table 5.11 Verification of the developed code [35]

Fiber orientation	$P_{failure}$ (MPa) (Numerical)	$P_{failure}$ (MPa) (Present)
$[\pm 90 / \pm 8.6_3 / \pm 90]$	164.5	160.72

5.3. Preliminary Study

Stacking sequences design of composite hydrogen storage vessels using stochastic optimization algorithms DE and NM was studied. Results of the preliminary study are presented in Table 5.12. Fiber orientation angles was considered as design variable. Thickness of a layer and liner, number of layers were constant.

Composite laminates were symmetric and balanced. Tsai-Wu, Tsai-Hill, Hashin Failure and Maximum Stress criteria were individually used to check whether the first ply failure was obtained in the laminates. Preliminary study considering three designs problems are shown in Table 5.12. Design problems A, B and C have 8, 12 and 16, number of layers, respectively. Mechanical and geometrical properties of designs were taken from the study (see Table 5.4) [20].

The optimization problem was defined as:

Find: $\{\theta_p, n\}, \theta_p \in [\theta_1, -\theta_1, \dots, \theta_n, -\theta_n]_s, \theta_p \in$ Integers,

p=1,2…,n where n=2,3 and 4 for separated designs

Minimize: Tsai-Wu, Tsai-Hill, Hashin Criterion, and Maximum Stress failure index

Constraints: Tsai-Wu≤ 1, Tsai-Hill ≤ 1, Hashin ≤ 1,

Maximum stress ≤ 1

$-90 \leq \theta_p \leq 90$

Symmetry

Balance

Methods: Differential Evolution, Nelder-Mead

Optimum angles and corresponding burst pressures obtained by DE method have approximated for Tsai-Wu and Tsai-Hill overall. However, this similarity hasn't been provided from the result of Tsai-Wu and NM algorithm. Oppositely, results obtained through Tsai-Hill, Hashin and Maximum Stress have been relatively more consistent in both algorithms. The deviation between the results of the optimization algorithms has been highest while using Tsai-Wu as failure constraint. Consequently, if one sets up constraints in the form of failure theories being especially Tsai-Wu in order to find optimum orientation and corresponding higher burst pressures, it would be better to use DE instead NM method. Besides, comparing CPU time, NM has showed better

performance than DE giving an exception to third design optimized using Tsai-Wu as a constraint.

Table 5.12 Optimization results of the preliminary study

Design	Failure Constraint	Optimum orientation DE	Burst Pressure (MPa) DE	Optimum orientation NM	Burst Pressure (MPa) NM	CPU time (sec) DE	CPU time (sec) NM
A	Tsai-Wu	$[\pm 55/\pm 54]_S$	9.67	$[\pm 62/\pm 47]_S$	8.91	5.8	4.7
	Tsai-Hill	$[\pm 54/\mp 54]_S$	9.59	$[\pm 54/\mp 53]_S$	9.52	6.3	4.6
	Hashin Failure	$[\pm 54_2]_S$	9.94	$[\pm 54/\pm 53]_S$	9.8	5.7	5.1
	Maximum Stress	$[\pm 52_2]_S$	11.1	$[\pm 52/\mp 52]_S$	11.1	6.4	5.1
B	Tsai-Wu	$[\pm 54/\pm 55_2]_S$	13.77	$\begin{bmatrix}\pm 90/\pm 42/\\ \mp 42\end{bmatrix}_S$	12.1	23.2	16.7
	Tsai-Hill	$[\pm 54_2/\mp 54]_S$	13.73	$\begin{bmatrix}\mp 52/\pm 59/\\ \pm 52\end{bmatrix}_S$	13.3	19.6	16.5
	Hashin Failure	$\begin{bmatrix}\pm 54/\mp 54/\\ \mp 53\end{bmatrix}_S$	14.19	$[\mp 54/\pm 53_2]_S$	14.24	13.6	9.5
	Maximum Stress	$[\mp 51/\pm 51_2]_S$	16.5	$[\mp 51/\pm 51_2]_S$	16.5	25.7	21.2
C	Tsai-Wu	$\begin{bmatrix}\mp 55/\mp 56/\\ \pm 53/\mp 56\end{bmatrix}_S$	17.5	$\begin{bmatrix}\mp 61/\mp 54/\\ \mp 46/\mp 53\end{bmatrix}_S$	16.3	35.2	39.9
	Tsai-Hill	$\begin{bmatrix}\mp 56/\pm 55/\\ \mp 51/\mp 53\end{bmatrix}_S$	17.38	$\begin{bmatrix}\mp 53/\mp 50/\\ \mp 60/\mp 53\end{bmatrix}_S$	17.1	27.8	26.3
	Hashin Failure	$\begin{bmatrix}\pm 55/\pm 52/\\ \pm 57/\mp 52\end{bmatrix}_S$	18.09	$\begin{bmatrix}\mp 56/\mp 49/\\ \mp 52/\mp 55\end{bmatrix}_S$	17.4	17.5	14.1
	Maximum Stress	$\begin{bmatrix}\mp 50/\mp 51_2/\\ \pm 51\end{bmatrix}_S$	21.28	$\begin{bmatrix}\mp 48/\mp 52_2/\\ \mp 53\end{bmatrix}_S$	19.8	38.3	37.7

In the aspect of failure constraints, Hashin failure criterion has been the quickest to give optimal results for both optimization algorithms. It should be noted that this might be observed due to relatively brief theoretical formulation of Hashin failure criterion which causes less workload on CPU.

5.3. Results and Discussions of the Design Problems

5.3.1. Design Problem I

The inner radius of Design I is 6.42 mm for 5 lt storage volume. The optimization results of the problem are listed in Table 5.13.

Table 5.13 Optimum solutions of Design I

Failure Constraint	Stacking Sequence DE	# of ply DE	Stacking Sequence NM	# of ply NM	CPU time DE (sec)	CPU time NM (sec)
Tsai-Wu	$[21]_S$	2	$[\pm 28 / \mp 43_2]_S$	12	3	16.5
Hashin-Rotem	$[\mp 28]_S$	4	$[\mp 2 / \pm 33 / \pm 34 / -39]_S$	14	4.1	19.4
Maximum Stress	$[\mp 27]_S$	4	$[\mp 2 / \mp 35 / \mp 10 / \pm 35]_S$	16	5.2	26.2

The results show that DE and NM have obtained different optimum solutions. The efficiency of NM in this design is below compared to DE with respect to required number of plies. Optimization has been performed by DE require only 2 composite plies to deliver design targets. Oppositely, NM has required 12 layers more to comprise design targets. Based on the optimization theory and studies done previously, optimization using Nelder Mead is generally quicker since it is a derivative free algorithm. However, this might change if the processed ply number or number of parameters to be processed will increase as occurred. In all criteria, more variety in helical layers has occurred by using NM with the requirement of more composite plies. Oppositely, DE only required one ply angle to accommodate design targets.

CPU times would not be comparable due to differently obtained plies. It should be noted that this problem design required minimum inner radius among other problem designs. Hence, it has less hoop and axial stresses. Optimum stacking sequences and number of layers obtained by using different failure criteria have been analogous. The number of plies required to comprise design targets has been minimum by using Tsai-Wu which also required less CPU time. On the other hand, partially interactive criteria; Hashin Rotem and non-interactive criteria; Maximum Stress, have nearly identical optimum solutions for both stacking sequence and number of plies. In addition,

optimum results have been attained by utilizing two failure modes for Hashin-Rotem; matrix and fiber failure and the failures of composite layers have occurred in both failure modes. The time and cost efficient method in optimizing first problem design is using DE with the incorporation of Tsai-Wu criterion.

5.3.2. Design Problem II

Radius of the pressure vessel design to be optimized has been found as 79.79 mm for 10 lt storage volume. The results for optimum stacking sequences and number of plies to accommodate design targets have been given in Table 5.14.

Table 5.14 Optimization results of Design II

Failure Constraint	**Stacking Sequence DE**	**# of ply DE**	**Stacking Sequence NM**	**# of ply NM**	**CPU time DE (sec)**	**CPU time NM (sec)**
Tsai-Wu	$[\mp 90_6]_S$	24	$[\pm 90/\mp 90/\pm 90_2/\mp 90/\pm 90]_S$	24	64.7	48.6
Hashin-Rotem	$[\pm 90/\mp 90/\pm 90_5]_S$	28	$[\mp 90_2/\pm 89_2/\mp 89/\pm 90_2]_S$	28	75.9	62.7
Maximum Stress	$[\pm 90/\mp 90/\pm 90_2/\mp 90_2/\pm 90]_S$	28	$[\mp 90/\mp 89/\pm 87/\pm 88/\mp 86/\pm 89/\pm 88]_S$	28	83.5	72.6

The results show that the discrepancy of optimum stacking sequence using DE and NM has been marginal. All fiber angles have been obtained in hoop direction (90^o) by using DE. However, optimum orientations obtained by using NM haven't included all plies in 90^o angle. Both algorithms have provided minimum numbers of plies when failure constraint was Tsai-Wu, similar to Design I. Fiber angle orientations have been analogous for all failure theories. The failure has occurred in fiber mode for Hashin-Rotem which is unlikely for Design I. Here, both algorithms have provided same ply numbers for each criterion. NM has been quicker than DE during optimizations of the design. For 10 lt storage volume vessel, it can be said that optimization process with using NM and Tsai-Wu has been the most efficient when cost and time are taken into consideration.

5.3.3. Design Problem III

Design III has inner radius of 112.94 mm to provide 20 lt storage volume. Optimum stacking sequences for this case has been indicated in Table 5.15.

Table 5.15 Optimization results of Design III

Failure Constraint	Stacking Sequence DE	# of ply DE	Stacking Sequence NM	# of ply NM	CPU time DE (sec)	CPU time NM (sec)
Tsai-Wu	$\left[\begin{matrix}\pm 90/\pm 72/\mp 72/\pm 72/\\ \mp 90/\mp 73/\mp 72_2/\pm 72/\\ \mp 72/-90\end{matrix}\right]_S$	42	$\left[\begin{matrix}\mp 73_2/\pm 73/\mp 83/\pm 73_2/\\ \pm 75/\mp 81/\mp 90/\mp 73/-88\end{matrix}\right]_S$	42	255.1	201.8
Hashin-Rotem	$\left[\mp 90_8/\pm 90_2/\mp 90\right]_S$	44	$\left[\begin{matrix}\mp 90_2/\pm 90/\mp 90/\pm 90_3/\\ \mp 90_3/\pm 90\end{matrix}\right]_S$	44	178.9	163.3
Maximum Stress	$\left[\begin{matrix}\mp 90/\pm 90/\mp 90/\pm 90/\\ \mp 90_6/\pm 90\end{matrix}\right]_S$	44	$\left[\begin{matrix}\mp 90/\mp 89/\pm 89/\mp 90/\\ \pm 89/\pm 90/\pm 88/\mp 89_4\end{matrix}\right]_S$	44	194.8	189.2

According to the results, optimizations obtained by using Tsai-Wu criterion have provided mostly helical layers. Oppositely, results obtained by using other criteria have provided mostly hoop layer. In addition, the number of plies has occurred as minimum for Tsai-Wu and it has been identical for the results obtained by using Hashin-Rotem and Maximum Stress similar to the solutions of previous designs. NM has generally required less CPU time as predicted. In this case, optimization performed using NM and Hashin-Rotem has been cost and time effective option.

5.3.4. Design Problem IV

Here, the radius of the pressure vessel to be optimized has been taken as 178.94 mm to provide 50 lt storage volumes. In Table 5.15, optimum stacking sequences obtained with the developed code has been given.

Table 5.16 Optimization results of Design IV

Failure Constraint	Stacking Sequence DE	# of ply DE	Stacking Sequence NM	# of ply NM	CPU time DE (sec)	CPU time NM (sec)
Tsai-Wu	$[\mp 2/\pm 71/\mp 90/\mp 20/\pm 90/\mp 86/\mp 74/\pm 90_2/\pm 66/\pm 90/\mp 42/\pm 88/\pm 82/\pm 56/\mp 90/\pm 15/\pm 90/\mp 49/\pm 57/\mp 12/\mp 90]_S$	88	$[\pm 15/\pm 1/\pm 75/\mp 73/\mp 72/\pm 88/\pm 52/\mp 33/\pm 80/\pm 71/\pm 35/\mp 68/\pm 72/\pm 56/\pm 83/\pm 78/\pm 83/\mp 71/\mp 77/\pm 45/\pm 85/\pm 53]_S$	88	1076	1023.9
Hashin-Rotem	$[\mp 3/\mp 90/\mp 16/\mp 90/\pm 90/\pm 69/\mp 90/\mp 57/\mp 23/\mp 71/\pm 65/\mp 90_3/\pm 90/\mp 90/\pm 39/\pm 90/\pm 73/\pm 90_2/\pm 43/\pm 50/\mp 14/\mp 64/\pm 5/-90]_S$	106	$[\pm 73/\mp 42/\mp 40/\pm 87/\pm 86/\mp 53/\mp 58/\pm 74/\pm 62/\mp 54/\mp 53/\mp 61/\pm 41/\pm 89/\mp 66/\mp 57/\mp 75/\mp 64/\pm 65/\mp 44/\pm 67/\mp 78/\pm 85/\pm 88/\mp 59/\pm 18/13]_S$	106	1398.2	1428.6
Maximum Stress	$[\mp 3/\mp 90/\mp 16/\mp 90/\pm 90/\pm 69/\mp 90/\mp 57/\mp 23/\mp 71/\pm 65/\mp 90_3/\pm 90/\mp 90/\pm 39/\pm 90/\pm 73/\pm 90_2/\pm 43/\pm 50/\mp 14/\mp 64/\pm 5/-90]_S$	106	$[\pm 84/\mp 80/\mp 10/\pm 76/\pm 85/\mp 50/\mp 62/\pm 82/\pm 62/\mp 24/\mp 64/\mp 28/\pm 61/\pm 79/\mp 86/\mp 60_2/\mp 27/\pm 77/\mp 62/\pm 88/\mp 70/\pm 57/\pm 80/\mp 66/\mp 33/83]_S$	106	1448.9	1487.1

According to the results, the behavioral difference of the algorithms is significant in each solution. The number of plies required has been minimum with Tsai-Wu compared to obtained results using other failure criteria, similar to previous designs.

Similar to Design II and Design III, there is no difference in number of plies of solutions obtained by both algorithms. The main difference in optimum stacking sequences is that the solutions obtained by using DE has included hoop angled layers but the solutions provided by NM hasn't included any hoop layers. DE has obtained similar stacking sequences for each failure criterion. Moreover, the optimum fiber orientations provided by using Hashin-Rotem and Maximum Stress have been identical. As oppose to this, discrepancy in stacking sequences obtained by NM has increased. It should be noted that, when it is said as hoop direction, only fiber angles being 90^o, has

been accepted as hoop direction. Otherwise, there have been angles being close to hoop direction. Along with the difference between hoop and helical layers, if stacking sequences have been compared to side to side, there has been no similarity between Tsai-Wu and other criteria.

CPU time has been minimum while using Tsai-Wu criterion which can be understandable. Since the number of plies which is required in obtaining optimum stacking sequence, has been the least among other failure theories. Apart from this, except for the results obtained by using Tsai-Wu, DE has been more efficient algorithm in determining the optimum stacking sequences which counters the general observations in literature. It might be said that, increment in workload might force the performance of algorithms differently. Otherwise, NM has been known its feature of finding solutions with less iteration. The most efficient algorithm and failure criterion have been NM and Tsai-Wu. It should be noted that NM algorithm features are set as default in optimization process. More advanced adjustment might positively affect the behavior of the algorithm.

According to optimization results for problem designs, increment in volume has directly affected stacking sequences when all design cases have been considered. First of all, number of plies obtained with each algorithm has been quite different in Design I. However, the number of plies in other designs is same when failure theories are taken into consideration individually. Both algorithms have obtained almost all layers in helical direction for design I, but in design II and design III, number of helical layers has been kept insignificant compared to hoop layers except for results obtained by using Tsai-Wu in Design III. The number of hoop layers has been significantly more than the hoop layers obtained by NM. Number of plies obtained by both algorithm, have been proportionally increased with volume. Since, increment in volume has been provided with enhancing inner radius of the vessels which increase axial and hoop resultant stresses. Moreover, it has been same by using Hashin-Rotem and Maximum Stress except Design I. Minimum number of plies has been obtained by using Tsai-Wu criterion for all cases. In each design, the variety of helical layers has been similar in solutions obtained by using Hashin-Rotem and Maximum Stress.

CPU time has been proved as being proportional with volume. Since, increment of volume results increment in number of iteration and plies. Moreover, constraints have been applied all layers which leads increasing in workload on CPU. Generally,

NM has been more cost effective than DE in obtaining solutions if obtained number of plies were same.

This study shows that small volume differences might affect directly optimum stacking sequences and increment in workload due to number of layers has been first reason causing abrupt changes in stacking sequences. Design IV have required 2.5 times more plies than Design III, 4 times more than design II and 44 times more than Design I and workload on CPU has been exponentially escalated that last design has required 6.6, 19.3, 105 times more time in obtaining solutions than Design III, Design II and Design I, respectively. In the situation of requirement for over 100 layers as obtained in Design IV, more helical layers have been employed to meet stress concentration. Moreover, analogous situation occurred for solutions having less than 20 layers (Design I). It should be noted that the volume increment has been provided by only one geometrical change; inner radius. However, volume can also be adjusted by length or both of them. Therefore, further studies on volume might reveal different deductions on optimum stacking sequence design. In addition to that, properties of the materials have been kept for all designs. Hence, studies with different composite systems might occur entirely different results. Comparison of the average of required number of plies with respect to change in volume and algorithm can be seen in Figure 5.2 and the comparison of average CPU time with respect to change in volume and algorithm has been indicated in Figure 5.3. In these figures, average values have consisted of failure theories in same manner. As can be seen in Figure 5.2, both algorithms have performed identical in obtaining the required number of layers in the vessel designs having same volume except Design I.

NM has been quicker than DE in obtaining solutions except Design I and Design IV as seen in Figure 5.3. The reason for NM falling behind DE in Design I is requiring more layers but for Design II and Design III, this behavior has reversed. In last design, DE obtained solutions quicker. According to these solutions, DE might prove its robustness and stability through increment in workload by delivering more hoop layers which has been known as ease in manufacturing while NM has been proved to be faster algorithm in general. Hence, it might provide major cost differences in optimization studies which especially cover large amount of parameter and workload.

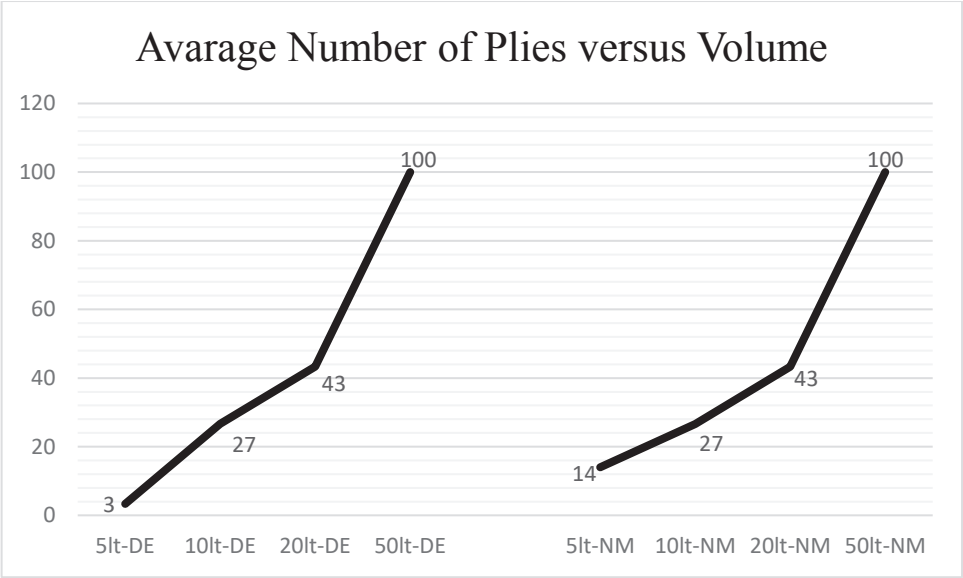

Figure 5.2 Comparison of the average number of plies versus volume

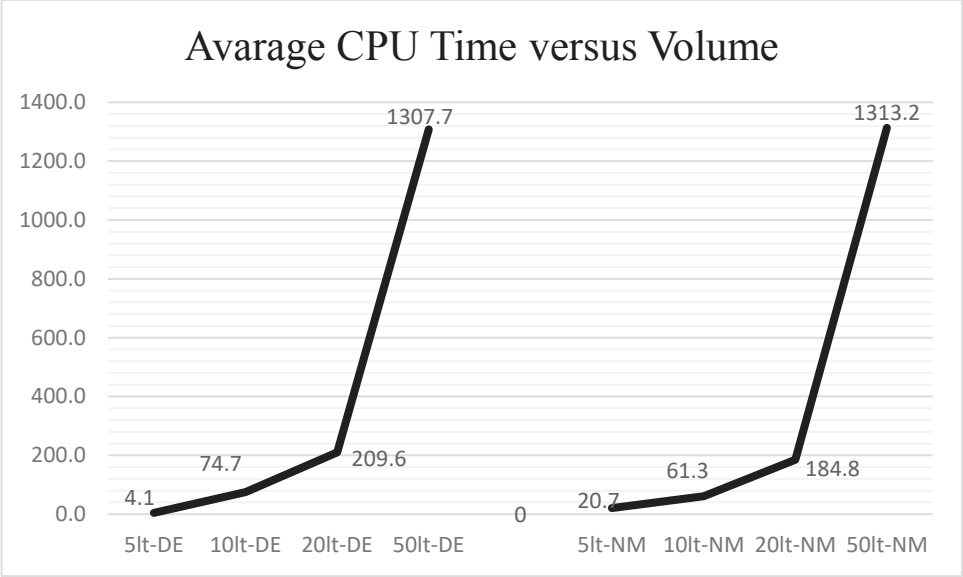

Figure 5.3 Comparison of the average CPU time versus volume

In this study, single objective stacking sequence optimization using DE and NM incorporating with three differently categorized failure theories has been investigated. Design targets have been achieved using both algorithms and failure theories. Mechanical behavior of designs might slightly differ if the plastic theory for liner is included. The problems have not been set to be example for manufacturing purposes. Therefore, algorithms have been asked to select fiber angles from integer ranging

between -90^{o} and 90^{o}. However, results might show that the stacking sequences obtained using DE might be more useful for manufacturing purposes due to obtaining more hoop layers which are known being easy to wind.

CHAPTER 6

CONCLUSION

This thesis has presented a study of the design of stacking sequences for laminated composite part of pressurized gas storage vessel by stochastic search algorithms. The vessel is subjected to internal pressure. This causes axial and hoop resultant loadings in composite layers and liner. In the development of pressure storage vessel, satisfying the conditions; high strength and lower weight has to be considered to provide safety regulations and weight restrictions for certain applications such as fuel cell vehicle. Composite pressurized hydrogen storage vessel with metal liner (Type III) can satisfy these requirements with a convenient stacking sequence of composite section. In order to design optimum laminated composite outer shell for a Type III storage vessel with such a stacking sequence, it is required to apply some of the optimization methods to composite design problems.

In this thesis, analysis and optimum stacking sequence design of composite hydrogen storage vessels with metal liner satisfying the conditions of first-ply failure at 1400 bar with minimum number of layers have been performed. Totally twenty-four optimization problems have been solved by using stochastic search algorithms Differential Evolution and Nelder Mead.

Failure criteria have been taken as the objective function to be minimized. Fiber angle orientation and number of laminated composite layers have been considered as design variables. Fiber angle orientation has been taken as angle-ply formation $\left[\pm\theta_1/.../\pm\theta_n\right]$ and symmetry of stacking sequence have been maintained for design problems considered. Four Type III cylindrical hydrogen storage vessel designs have been considered. Material properties, thickness of a ply and thickness of liner have been kept as constant for design problems. Carbon fiber reinforced epoxy is selected as composite part and liner material is selected as aluminum 6061-T6 alloy. The only difference between designs has been volume which was provided by adjusting inner radius. The storage vessels with 5, 10, 20 and 50 liters have been considered for the specified problems Design I, Design II, Design III and Design IV, respectively. Designs don't conflict with thin-walled cylindrical pressure vessel analysis based on CLT. A computer code based on CLT employing failure theories and optimization algorithms

has been developed by using Wolfram MATHEMATICA Commercial Software. Verification of the developed code have been performed with certain studies from the literature. Single objective optimization has been performed with number of constraints; failure index of all plies has been asked to be lower or equal than 1, fiber angle orientations have been asked to be chosen from integers and ranged between -90^o and 90^o. Three different failure approaches have been considered being Tsai-Wu as interactive theory, Hashin-Rotem as partially interactive theory and Maximum Stress as non-interactive criterion. Other objective of the study has been to reveal the effect of volume differences on fiber orientation angle and number of plies in cylindrical composite pressure vessels.

The most significant difference has been observed in 5 lt volume vessel design (Design I). The main difference has been in number of plies obtained by algorithms. Although DE was able to satisfy design targets with just 2 plies with Tsai-Wu, 4 plies with Hashin-Rotem and Maximum Stress, NM required at least 12, 14 and 16 plies for failure constraints, respectively, to satisfy the failure strength. The second highlight of the optimal solutions of this problem design has been that, for all criteria and algorithms, fiber orientation angles were in helical directions. In Design II, required number of plies for algorithms was same for certain failure criterion and optimum solutions obtained by minimizing Tsai-Wu required less composite plies. Fiber orientation angle which is determined by NM, included more helical layers but DE obtained all angle in hoop direction. Moreover, evolution time of optimizations performed by NM is less than DE. The same condition about number of plies and CPU time has also been valid for the optimum solutions of Design III. Apart from this, results obtained with Tsai-Wu included more helical layers. However, other two criteria behaved similar and included mostly hoop layers. The other important stacking sequence design difference occurred in Design IV. Since, all solutions have included the most variable fiber orientation angles among designs ranging from 2^o to 90^o. The algorithm behaviors with respect to number of plies and failure criteria were similar with Design II and Design III. Further, NM was only quicker in optimization with Tsai-Wu criterion which is obtained differently in other designs.

The difference in volume between the pressure vessels has induced disturbance and variety for multiple aspects. The optimizations performed by Hashin-Rotem and Maximum Stress gave similar results. Similarly, fiber orientation angles and number of plies were obtained identical by DE algorithm. Secondly, NM seemed to lose its

capability in giving solutions in the aspect of required number of plies when the workload was narrow (Design I) and the speed in obtaining solutions for designs which involve number of composite layers larger than 100 (Design IV). Fiber orientation angles through designs vary. Despite the fact that any hoop layers haven't occurred in Design I. Both Design II and Design III only included hoop layers. On the other hand, solutions of Design IV included both helical and hoop layers in variety. Further, volume differences affected required number of layers and CPU time exponentially. For example, Design II had twice the volume of Design I. However, Design II required 12 times more plies (DE and Tsai-Wu) and 21 times more CPU time. On the other hand, although the volume ratio between Design II and Design III is 2, required number of plies of Design III over Design II is 1.75. However, their CPU time ratio became 4 (DE and Tsai-Wu). The volume ratio between Design IV and Design III is 2.5. Ratio of required number of plies has been 2.1 and ratio of required CPU time has been 4.2 (DE and Tsai-Wu). According to the results, it can be said that increment in volume has exponentially increased when compared to required number of plies of optimum solutions.

REFERENCES

[1] Panwar, N.L., Kaushik, S.C., Kothari, S. Role of renewable energy sources in environmental protection: a review. Renewable and Sustainable Energy Revolution, (2011), 15:1513-24

[2] Bundesministerium für Wirthshaft und Technologie. Die Energiewende zum Erfolg führen, (2015). http://www.bmwi.de/Redaktion/EN/Dossier/energy-transition.html

[3] Smeets, F., Vaes, J., Zhang, D., Zeng, K., Tjarks, G., H2 from Electricity. In Hydrogen Science and Engineering: Materials, Processes, Systems and Technology, ed. D Stolten, B Emonts, (2016), pp. 253–390.

[4] Tremel, A., Wasserscheid, P., Baldauf, M., Hammer, T., Techno-economic analysis for the synthesis of liquid and gaseous fuels based on hydrogen production via electrolysis. Int. J. Hydrogen Energy, (2015), 40:11457–64.

[5] Stolten, D., Emonts, B., Hydrogen Science and Engineering: Materials, Processes, Systems and Technology. (2016), vol. 2.

[6] Topler, J. and Lehman, J., Hydrogen and Fuel Cell: Technologies and Market Perspectives. Berlin:Springer, (2014)

[7] Grote, J-P, Zeradjanin, A.R., Cherevko, S., Savan, A., Breitbach, B., Screening of Material Libraries for Electrochemical CO Reduction Catalysts – Improving Selectivity of Cu By Mixing with Co. J. Catal., (2016), 343:248–56.

[8] Jones, L.W., Perspectives on the Evolution into A Hydrogen Economy. Energy Community, (1976), 2(6):573–84.

[9] Pasini, J.M., Corgnale, C., van Hassel, B.A., Motyka, T., Kumar, S., Simmons, K.L., Metal hydride material requirements for automotive hydrogen storage systems. Int. J. Hydrogen Energy, (2013), 38(23):9755–65.

[10] US Department of Energy, Technical Assessment: Cryo-Compressed Hydrogen Storage for Vehicular Applications. Washington, DC: U.S. Dep. Energy Hydrogen Prog., US Dep. Energy, (2008), https://www.hydrogen.energy.gov/pdfs/cryocomp_report.pdf.

[11] Kunze, K., Kirchner, O., Cryo-compressed hydrogen storage. Presented at Cryogenic Cluster Day, Sep. 28, Oxford, UK, (2012), https://www.stfc.ac.uk/stfc/cache/file/F45B669C-73BF-495BB843DCDF50E8B5A5.pdf.

[12] Ahluwalia, R., Hua, T., Peng, J., Lasher, S., McKenne, K., Sinha, J., Technical Assessment of Cryocompressed Hydrogen Storage Tank System For Automotive Applications. Int. J. Hydrogen Energy, (2010), 35:4171–84.

[13] Durbin, D.J. and Jugroot, C.M., Review of hydrogen storage techniques for on board vehicle applications. International Journal of Hydrogen Energy, (2013), 1-23.

[14] Hua, T., Ahluwalia, R., Peng, J.K., Kromer, M., Lasher, S., McKenney, K., Law, K., Sinha, J., Technical Assessment of Compressed Hydrogen Storage Tank Systems for Automotive Applications. US Department of Energy, (2010).

[15] Lee, S., Ed., Handbook of Composite Reinforcements. Wiley-VCH, (1993).

[16] Vasiliev, V.V. and Morozov, E.V., Mechanics and Analysis of Composite Materials. New York, NY: Elsevier, (2001).

[17] Tauchert, T.R., Optimum design of a reinforced cylindrical pressure vessel. Journal of Composite Materials. (1981), 15, pp.390-402.

[18] Reddy, J.N., Pandey, A.K., A First-ply failure analysis of composite laminates. Computers & Structures, (1987), 25(3), pp.371-93.

[19] Reddy, Y.S.N. and Reddy, J.N., Linear and non-linear failure analysis of composite laminates with transverse shear. Journal of Computer Science and Technology, (1992), 44, pp.227-55

[20] Chang, R. R., Experimental and theoretical analyses of first -ply failure of laminated composite pressure vessels. Composite Structures, (2000), 49, 237-243.

[21] Park, J.H, Hwang, J.H, Lee, C.S., Hwang, W., Stacking Sequence Design of Composite Laminates for Maximum Strength using Genetic Algorithms. Composite Structures, (2001), 52, pp.217-231.

[22] Kabir, M., Finite Element Analysis of Composite Pressure Vessels with a Load Sharing Metallic Liner. Composite Structures, 49, (2000), pp.247-255.

[23] Kim, C.U., Kang, J.H., Hong, C.S., Kim, C.G., Optimal Design of Filament Wound Structures under Internal Pressure based on the Semi-Geodesic Path Algorithm. Composite Structures, 67, (2005), pp. 443-452.

[24] Chapelle, D. and Perreux, D., Optimal design of a Type 3 hydrogen vessel: Part I—Analytic modelling of the cylindrical section. International Journal of Hydrogen Energy, 31, (2006), 627-638.

[25] Pelletier, J.L. and Vel, S.S., Multi-objective optimization of fiber reinforced composite laminates for strength, stiffness and minimal mass. Computer and Structures, 84, (2006), 2065-2080.

[26] Deb, K., Multi-objective optimization using evolutionary algorithms. John Wiley and Sons Ltd. (2001).

[27] Deb, K., A fast and elitist multi-objective genetic algorithm NSGA-II. IEEE Trans Evolution Computer, 6(2), (2002), 182–96.

[28] Zheng, J.Y., Liu, P.F., Elasto-plastic stress analysis and burst strength evaluation of Al-carbon fiber/epoxy composite cylindrical laminates. Computational Materials Science, 42(3), (2008), 453-461.

[29] Xu, P., Zheng, J.Y., Liu, P.F., Finite element analysis of burst pressure of composite hydrogen storage vessels. Materials and Design, 30, (2009), 2295-2301.

[30] Liu, P.F., Xing, L.J., Zheng, J.Y., Failure analysis of carbon fiber/epoxy composite cylindrical laminates using explicit finite element method. Composites: Part B, 56, (2014), 54-61.

[31] Gentilleau, B., Bertin, M., Touchard, F., Grandidier, J.C., Stress analysis in specimens made of multi-layer polymer/composite used for hydrogen storage application: Comparison with experimental results. Composite Structures, 93, (2011), 2790-2767.

[32] Ghouaoula, A., Hocine, A., Chapelle, D., Karaachira, F., Boubakar, M. L., Analytical prediction of damage in the composite part of a Type-3 hydrogen storage vessel. Mechanics of Composite Materials, 48, (2012).

[33] Francescato, P., Gillet, A., Leh, D., Saffre, P., Comparison of optimal design methods for Type 3 high-pressure storage tanks. Composite Structures, 94, (2012), 2087–2096.

[34] Kumar, S.S, Kumari, A.S., Design and Failure analysis of Geodesic Dome of a Composite Pressure vessel. IJERT, 1, (2012).

[35] Alcantar, V., Ledesma, S., Aceves, S.M., Ledesma, E., Saldana, A., Optimization of Type III pressure vessels using genetic algorithm and simulated annealing. International Journal of Hydrogen Energy, 42, (2017), 20125-20132.

[36] Xu, P., Zheng, J., Chen, H., Liu, P., Optimal design of high pressure hydrogen storage vessel using an adaptive genetic algorithm. International Journal of Hydrogen Energy, 35(7), (2010), 2840-2846.

[37] Alcantar, V., Aceves, S.M., Ledesma, E., Ledesma, S., Aguilera, E., Optimization of Type 4 composite pressure vessels using genetic algorithms and simulated annealing. International Journal of Hydrogen Energy, 42, (2017), 15770-15781.

[38] Roh, H., Hua, T., Ahluwalia, R., Optimization of carbon fiber usage in Type 4 hydrogen storage tanks for fuel cell automobiles. International Journal of Hydrogen Energy, 38(29), (2013), 12795-12802.

[39] Kaw, A. K., Mechanics of Composite Materials. 2nd edition, CRC Press Taylor & Francis Group, (2012).

[40] Akbulut, U., Çimento ve Betonun Tarih İçinde Gelişimi, (2012).

[41] Nagayama, K., The Connoisseur's Book of Japanese Swords. Kodansha International, (1997), p. 49. ISBN 4-7700-2071-6.

[42] Clive, S., Samurai: The Weapons and Spirit of the Japanese Warrior, Lyons Press, (2004), pp. 40–58. ISBN 978-1-59228-720-8.

[43] Vinson, J. R., and Sierakowski, R. L., The Behavior of Structures Composed of Composite Materials. Kluwer Academic Publishers, (2004).

[44] Ogale, V. and Alagirusamy, R., Textile Preforms for Advanced Composite Review Article. Indian Journal of Fibre and Textile Research, (2004), vol.29: 366-375.

[45] CarbonFiber, Web Article, (2014), http://www.carbonfiber.gr.jp/english/material/type.html

[46] Prashanth, S., Subbaya, K.M., Nithin, K., Sachhidananda, S., Fiber Reinforced Composites – A Review, Prashanth et. al., Journal of Material Science and Engineering, (2017), 6:3, DOI: 10.4172/2169-0022.1000341.

[47] Shah, D. U., Schubel, P. J., Licence, P., & Clifford, M. J., Hydroxyethylcellulose Surface Treatment of Natural Fibres: The New "Twist" in Yarn Preparation and Optimization for Composites Applicability. Journal of Materials Science, (2012), 47(6), 2700–2711. https://doi.org/10.1007/s10853-011-6096-1.

[48] Wambua, P., Ivens, J., & Verpoest, I., Natural fibres: Can they replace glass in fibre reinforced plastics? Composites Science and Technology, (2003), 63(9), 1259–1264. https://doi.org/10.1016/S0266-3538(03)00096-4

[49] Faruk, O., Bledzki, A. K., Fink, H. P., & Sain, M., Bio-composites reinforced with natural fibers: 2000-2010. Progress in Polymer Science, (2012), https://doi.org/10.1016/j.progpolymsci.2012.04.003.

[50] Carbon Fiber Report, Composites World's Annual Carbon Fiber Conference, (2016), https://www.compositesworld.com/articles/carbon-fiber-2016-report

[51] Global and China Aramid Fiber Industry Report, (2017) https://www.reportlinker.com/p02515745/Global-and-China-Aramid-Fiber-Industry-Report.html

[52] Howarth, J., Mareddy, S. S. R, Mativenga, P. T., Energy Intensity and Environmental Analysis of Mechanical Recycling of Carbon fiber Composite. Journal of Cleaner Production, (2014), 1-5.

[53] Jiang, G., Pickering, S.J., Lester, E.H., Turner, T.A., Wong, K.H., Warrior, N.A., Characterization of Carbon fibres Recycled from Carbon fibre/Epoxy Resin Composites using Supercritical N-Propanol. Compos. Sci. Technol. (2009), 69, 192-198.

[54] Martin T. R., Meyer, S. W., Luchtel, D. R., An Evaluation of The Toxicity of Carbon Fiber Composites for Lung Cells in Vitro and in Vivo. Environmental Research, (1989), 49(2):246-61.

[55] Ansell, M., Natural Fibre Composites & Their Role in Engineering. University of Bath, (2011), Bio-composite Materials for Construction.

[56] Yuyan, L., LI, L., Linghui, M., The Experimental Research on Recycling of Aramid Fibers by Solvent Method. Journal of Reinforced Plastics and Composites, (2009), 28:2211.

[57] Mohanty, A. K., Misra, M., Hinrichsen, G., Biofibres, Biodegradable Polymers and Biocomposites: An Overview. Macromolecular Materials and Engineering, (2000), 1-24, 276-277.

[58] Marsh, J.P., Mossman, B.T., Driscoll, K.E., Schins, R.F., Borm, P.J., Effects of Aramid, a high strength synthetic fiber, on respiratory cells in vitro. Drug and Chemical Toxicology, (1994), 17(2):75-92.

[59] Kyocera Corporation, Characteristics of Fine Ceramics, https://global.kyocera.com/fcworld/charact/strong/hardness.html.

[60] Daniel, I. M., & Ishai, O., Engineering Mechanics of Composite Materials. (2005), https://doi.org/10.1016/B978-0-08-006421-5.50049-6.

[61] Pirolini, A., Materials Used in Space Shuttle Thermal Protection Systems. Web article, (2014), https://www.azom.com/article.aspx?ArticleID=11443.

[62] Hallett, R., Giant TCR Advanced SL Review, web article, sourced from Giant-bicycles.com, (2012), https://cycletechreview.com/2012/reviews/giant-tcr-advanced-sl-road-test/7.

[63] Zorn and Walter, Speed and Power Calculator, (2015), http://www.kreuzotter.de/english/espeed.htm.

[64] Shama, R.N., Simha, T.G.A., Rao, K.P., Ravi, K.G.V.V., Carbon Composites are Becoming Competitive and Cost Effective. (2017), white paper, Infosys Limited.

[65] Carus, M., Bio-composites: technologies, applications and markets, 4th International Conference on Sustainable Materials, Polymers and Composites, (2011).

[66] Schlapbach, L. and Zuttel, A. Hydrogen storage materials-mobile applications. Nature, 414, (2001), pp. 353-358.

[67] Sandrock, G., Hydrogen Metal Systems and Applications of Hydrides, in Hydrogen Energy Systems. Production and Utilization of Hydrogen and Future Aspects, Y. Yurum, ed. (1995), pp. 135-166.

[68] Borel, J.P., Thermodynamical Size Effect and The Structure of Metallic Clusters. Surface Science, 106, (1981), pp.1–9.

[69] Nishimura, C., Komaki, M., and Amano, M., Hydrogen Permeation through Magnesium. Journal of Alloys and Compounds, 293, (1999), pp.329–333.

[70] Ge, Q., Structure and Energetics of LiBH4 and its Surfaces: A First-Principles Study. The Journal of Physical Chemistry A, 108, (2004), pp.8682–8690.

[71] Zaluska, A., Zaluski, L., and Strom Olsen, J.O., Nanocrystalline Magnesium for Hydrogen Storage. Journal of Alloys and Compounds, 288, (1999), pp.217–225.

[72] San, M.C., Dedrick, D.E., Van, B.P., Somerday, B.P., Nibur, K.A., Pressure Cycling of Type I Pressure Vessels with Gaseous Hydrogen. Sandia National Laboratories, (2012)

[73] European Integrated Hydrogen Project, (EIHP), http://www.eihp.org

[74] Irani, R.S., Hydrogen Storage: High-Pressure Gas Containment. MRS Bulletin, Vol. 27, No. 9, (2002), pp. 680-682.

[75] Barthelemy, H., Weber, M., Barbier, F., Hydrogen Storage: Recent İmprovements and Industrial Perspectives. International Journal of Hydrogen Energy, (2016), pp.1-9.

[76] US Department of Energy, (a)http://energy.gov/eere/fuelcells/doe-technical-targetsonboard-hydrogen-storage-light-duty-vehicles. (b)http://energy.gov/eere/fuelcells/doe-technical-targets-onboardhydrogen-storage-light-duty-vehicles, (2015).

[77] Ren, J., Musyoka, N.M, Langmi, H.W., Mathe, M., Liao, S., Current research trends and perspectives on materials-based hydrogen storage solutions: A critical review. International Journal of Hydrogen Energy xxx, (2016), pp.1-23.

[78] Mallick, P.K., Fiber-Reinforced Composites: Materials, Manufacturing and Design. 3rd edition, (2007), p.65-69.

[79] Bert, C.W., Classical Lamination Theory, Section IIB, (1989).

[80] Hinton, M.J., Kaddour, A.S., Soden, P.D., The Word-Wide Failure Exercise: Its origin, concept and content. Failure Criteria in Fibre Reinforced Polymer Composites, (2004), p.11-15.

[81] Daniel, I. M., and Ishai, O., Engineering mechanics of composite materials. Oxford, England: Oxford University Press, (1994).

[82] Vinson, J.R. and Sierakowski, R.L., Introduction to Composite Materials. In: The behavior of structures composed of composite materials. Mechanics of Structural Systems, 5, (1987), p. 1-2.

[83] Hibbeler, R.C., Mechanics of Materials. 8th Edition, (2011), p. 405-407

[84] Gere, J.M., Mechanics of Materials. 6th Edition, (2004), p. 548-5

[85] Aydin, L., and Artem, H. S., Comparison of stochastic search optimization algorithms for the laminated composites under mechanical and hygrothermal loadings. Journal of Reinforced Plastics and Composites, 30(14), (2011), 1197–1212.

[86] Gurdal, Z., Haftka, R. T., & Hajela, P., Design and optimization of laminated composite materials. John Wiley & Sons, (1999).

[87] Rao, S. S., Engineering Optimization: Theory and Practice. Wiley, (2009). https://doi.org/10.1002/9780470549124

[88] Storn, R., & Price, K. Differential Evolution – A Simple and Efficient Heuristic for global Optimization over Continuous Spaces. Journal of Global Optimization, 11(4), (1997), 341–359. https://doi.org/10.1023/A:1008202821328

[89] Sivanandam, S. N., & Deepa, S. N. Introduction to Genetic Algorithms. Introduction to Genetic Algorithms. Berlin, Heidelberg: Springer Berlin Heidelberg, (2008). https://doi.org/10.1007/978-3-540-73190-0

[90] Roque, C. M. C., & Martins, P. A. L. S., Differential evolution optimization for the analysis of composite plates with radial basis collocation meshless method. Composite Structures, 124, (2015), 317–326. https://doi.org/10.1016/j.compstruct.2015.01.019

[91] Nelder, J. A., & Mead, R., A simplex-method for function minimization. Computer Journal, 7(4), (1965), 308–313. https://doi.org/10.1093/comjnl/7.4.308.

[92] Fan, S.-K. S., Liang, Y.-C., Zahara, E., A Genetic Algorithm and a Particle Swarm Optimizer Hybridized with Nelder-Mead Simplex Search. Computers and Industrial Engineering, (2006), 401–425.

[93] Vo-Duy, T., Ho-Huu, V., Do-Thi, T. D., Dang-Trung, H., Nguyen-Thoi, T., A global numerical approach for lightweight design optimization of laminated composite plates subjected to frequency constraints. Composite Structures, 159, (2017), 646–655.

[94] Barati, R., Parameter estimation of nonlinear muskingum models using nelder-mead simplex algorithm. Journal of Hydrologic Engineering, 19, (2011), 1–8.

[95] Wolfram Research, Inc., Mathematica, Version 11, Champaign, IL, (2018).